NMR Studies of the Secondary Structure in Solution and the Steroid Binding Site of Δ^5-3-Ketosteroid Isomerase in Complexes with Diamagnetic and Paramagnetic Steroids†

Qinjian Zhao,‡,§ Chitrananda Abeygunawardana,‡ and Albert S. Mildvan*,‡

Department of Biological Chemistry and Department of Pharmacology and Molecular Sciences, The Johns Hopkins University School of Medicine, Baltimore, Maryland 21205

Received November 18, 1996; Revised Manuscript Received January 22, 1997⊗

ABSTRACT: Backbone and side chain resonances of steroid-bound Δ^5-3-ketosteroid isomerase (EC 5.3.3.1), a homodimeric enzyme with 125 residues per monomer, have been assigned by heteronuclear NMR methods with the ^{15}N- and ^{13}C-labeled enzyme. The secondary structure in solution of steroid-bound isomerase, based on interproton NOE's and differences in chemical shifts of backbone Hα, Cα, Cβ, and CO resonances from random coil values, consists of two α-helices (residues 5−21, 48−60), one 3_{10} helix (residues 23−30), seven β-strands (residues 34−38, 44−47, 62−67, 71−73, 78−87, 92−104, and 111−116), and five turns (residues 39−42, 74−77, 88−91, 105−108, and 119−122). Thus isomerase consists of 30% helix, 38% β-sheet, and 16% turns. The remaining 20 residues (16%) are assumed to form coils. With the exception of a parallel interaction between β-strands 1 and 7, all β-strand interactions are antiparallel, forming both a β-hairpin (β1, β2) and a four-stranded β-sheet in which the first strand is interrupted (β3−β4, β5, β6, β7). ^{1}H−^{15}N HSQC titrations of the free enzyme with the substrate analog 19-nortestosterone hemisuccinate revealed steroid-induced changes in backbone ^{15}N and NH chemical shifts throughout the enzyme, with maximal effects on helix 1 (Val-15), β-strand 1 of the β-hairpin (Asp-38), the loop between helix 3 and β-strand 3 (Leu-61), β-strand 3 (Ala-64), β-strand 5 (Phe-82, Ser-85, Glu-87), β-strand 6 (Ile-98), and β-strand 7 (Ala-114, Phe-116) of the β-sheet, thus indicating the secondary structural components involved in steroid binding. These effects include regions near the catalytic residues Tyr-14 and Asp-38 which function as the general acid and base, respectively, in the ketosteroid isomerase reaction. Intermolecular NOE's between 19-nortestosterone hemisuccinate and isomerase indicate that the steroid binds near α-helices 1 and 3, which form one wall of the active site, and one end of the four-stranded β-sheet which forms the other wall. Consistent with these observations, doxyldihydrotestosterone, a steroid that is spin-labeled at its solvent-exposed end [Kuliopulos, A., Westbrook, E. M., Talalay, P., & Mildvan, A. S. (1987) *Biochemistry 26*, 3927−3937], induced the selective attenuation in the ^{1}H−^{15}N HSQC spectra of cross peaks of residues at the end of helix 3 (Ser-58, Leu-59, Lys-60, Leu-61), β-strand 5 (Val-84, Ser-85), and β-strand 6 (Val-95), due to the proximity of the nitroxide radical to the backbone ^{15}N and NH nuclei of these residues, thus confirming the location of the D ring of the bound steroid and defining the mouth of the active site.

Δ^5-3-Ketosteroid isomerase from *Pseudomonas testosteroni* (EC 5.3.3.1), a homodimeric enzyme with 125 amino acids per subunit, catalyzes the conversion of Δ^5- to Δ^4-3-ketosteroids via a dienolic intermediate (Xue et al., 1991; Eames et al., 1990; Holman & Benisek, 1994; Zhao et al., 1996b), accelerating the rate of this reaction by a factor of $\sim 10^{10}$ (Kuliopulos et al., 1990). The reaction mechanism involves concerted general acid/base catalysis by Tyr-14 and Asp-38, respectively (Kuliopulos et al., 1989, 1990; Xue et al., 1990) (Figure 1). In the enolization step of the reaction, Asp-38 deprotonates C-4 of the substrate, with a significant tunneling contribution to the proton transfer (Xue et al., 1990), as Tyr-14 donates a strong, low-barrier hydrogen bond to the developing dienolic intermediate (Zhao et al., 1995a, 1996a,b). In the reketonization step of the reaction, Asp-38 protonates C-6 of the intermediate to form the product while the interaction with Tyr-14 weakens to a conventional hydrogen bond (Figure 1).

While much is known about the intimate mechanism of the isomerase reaction, the structural basis for this mechanism is incompletely understood. Although the enzyme was already crystallized in 1960 (Kawahara & Talalay, 1960), the X-ray structure of the enzyme (Westbrook et al., 1984; Kuliopulos et al., 1987b) could not be refined to an *R*-factor below 35%, a problem ascribed to the unfavorably long *c*-axis of the hexagonal unit cell with a $P6_122$ space group and the presence of 48 monomers of isomerase per unit cell. For this reason, we have begun to examine the solution structure of this enzyme.

The present paper describes the secondary structure, in solution, of the Y55F/Y88F highly active mutant of isomerase, when complexed with 19-nortestosterone hemisuccinate (19-NTHS).[1] This mutant, in which two nonessential tyrosine

† These studies were supported by NIH Grants DK 07422 (to Paul Talalay) and DK 28616 (to A.S.M.). Q.Z. was supported by a fellowship from the National Cancer Institute (5T32 CA09243).

* Corresponding author.
‡ Department of Biological Chemistry.
§ Department of Pharmacology and Molecular Sciences.

⊗ Abstract published in *Advance ACS Abstracts,* March 1, 1997.

S0006-2960(96)02844-9 CCC: $14.00

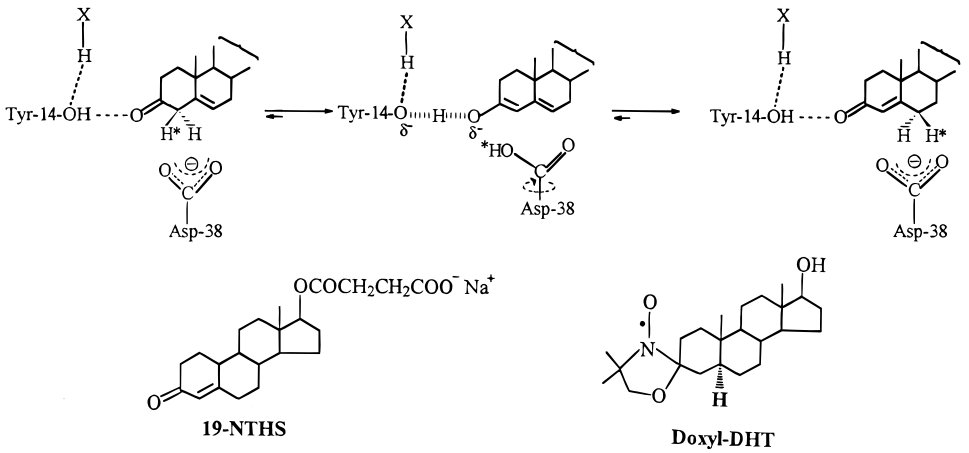

FIGURE 1: Catalytic mechanism of isomerase in which Asp-38 and Tyr-14 function as general base and acid, respectively, showing a low-barrier hydrogen bond between isomerase and the intermediate (Zhao et al., 1996b). Also shown are the structures of the steroids 19-NTHS and doxyl-DHT used in these studies.

residues (Tyr-55 and Tyr-88) have been replaced by phenylalanine, retains Tyr-14 as the only tyrosine residue. It shows 80% of the activity of the wild-type enzyme when expressed as k_{cat}/K_m (Kuliopulos et al., 1991) and was found to be more soluble than the wild-type enzyme. The steroid, 19-NTHS, is a more soluble analog of 19-nortestosterone and is also a competitive inhibitor and substrate of the reverse isomerase reaction (Wang et al., 1963). In addition, the introduction of an ester group at the 17β-position minimizes backward binding (Schwab & Henderson, 1990). Thus, by use of this steroid as ligand we have defined, by chemical shift changes and intermolecular nuclear Overhauser effects, the environment of the enzyme-bound steroid in the normal binding mode for catalysis. As an independent determination of the location of the active site, paramagnetic effects of doxyl-DHT, a spin-labeled steroid competitive inhibitor, on the $^1H-^{15}N$ HSQC spectrum of the enzyme were also studied. An abstract from the laboratory of R. M. Pollack describing preliminary NMR studies of the solution structure of *free* wild-type isomerase states that the enzyme contains 25% helix and 70% β-sheet (Ebrahimian et al., 1995).

EXPERIMENTAL PROCEDURES

Materials. 19-Nortestosterone hemisuccinate (19-NTHS) was synthesized as reported (Kuliopulos et al., 1991). Doxyl-DHT and sodium ascorbate were obtained from Aldrich (St. Louis, MO). Ammonium sulfate, ampicillin, IPTG, glucose, NH_4Cl, DMSO-d_6, MOPS, and Tricine were purchased from Sigma (St. Louis, MO). [^{13}C]Glucose and [^{15}N]NH_4Cl from Cambridge Isotope Laboratory (Andover, MA) were used for uniform labeling of the Y55F/Y88F mutant in MOPS medium (Zhao et al., 1996a).

Expression and Purification of Labeled Isomerase. The Y55F/Y88F double mutant of isomerase, which has 80% of the activity of the wild-type enzyme as measured by k_{cat}/K_M (Kuliopulos et al., 1991), was used for these studies. *Escherichia coli* BL21 DE3 (Novagen, Madison, WI) transformed with pET-25b(+) expression vector carrying the Y55F/Y88F mutant isomerase gene (Zhao et al., 1996a) was grown in 1 L of MOPS medium (Neidhardt et al., 1974), supplemented with 2 g of ^{13}C-labeled glucose (or unlabeled glucose as needed) and/or 1 g of ^{15}N-labeled NH_4Cl. Single colonies were used to inoculate 20 mL of LB medium containing ampicillin (100 μg/mL). When the absorbance at 600 nm reached 1.5, the bacteria were centrifuged at 1000*g* for 5 min, resuspended in the above-mentioned MOPS medium, and used to inoculate 1 L of MOPS medium. Bacteria were grown at 28 °C, and when A_{600} reached 0.8−1.0, 1 mM IPTG was added to induce protein expression. After centrifugation, the pellet was subjected to three cycles of freezing over dry ice and thawing in a water bath at room temperature. The bacteria were then resuspended in 50 mL of a 50 mM Tris-HCl and 100 mM NaCl buffer solution, pH 7.5, and sonicated at 4 °C for three 10 s periods. After removal of the supernatant fraction by centrifugation, the pellet was again resuspended and sonicated. The supernatant fractions were combined and Polymin P was added to a final concentration of 0.8% (w/v) to precipitate nucleic acids. After centrifugation, ammonium sulfate was added to the supernatant fraction to 85% saturation to precipitate the isomerase. The mutant isomerase was purified to electrophoretic homogeneity and crystallized as described (Kuliopulos et al., 1989, 1991; Zhao et al., 1996a), except that a Phenyl-Sepharose (fast flow, high substitution; Pharmacia) column (2.5 cm × 15 cm) was employed in place of the ion-exchange chromatography. The crude isomerase solution was loaded onto the column in 50 mM sodium phosphate buffer and 0.5 M NaCl, pH 7.2 (buffer A) and eluted with a linear gradient to 100% buffer B (5 mM sodium phosphate, pH 7.2, in 50% ethanol). The purity of the fractions containing isomerase (which eluted at 17% ethanol) was checked by SDS−PAGE and UV spectra. The fractions which were at least 90% pure were pooled and concentrated with Centri-Prep-10 cartridges (Amicon) which have a molecular mass cutoff of 10 kDa. The concentrated isomerase solutions were subjected to three dilution/concentration cycles to remove the ethanol, and the enzyme was then crystallized by addition

[1] Abbreviations: DMSO-d_6, perdeuterated dimethyl sulfoxide; doxyl-DHT, doxyldihydrotestosterone, spiro[doxyl-2,3′-5′α-androstan]-17β-ol, or 3-doxyl-17β-hydroxy-5α-androstane; FID, free induction decay; HSQC, heteronuclear single-quantum correlation; HMQC, heteronuclear multiple-quantum correlation; isomerase, Δ^5-3-ketosteroid isomerase (EC 5.3.3.1); Y55F/Y88F, mutant isomerase in which Tyr-55 and Tyr-88 have been replaced by phenylalanine (all references to isomerase in this paper are to this mutant, unless otherwise stated); NMR, nuclear magnetic resonance; MOPS, 3-(*N*-morpholino)propanesulfonic acid; IPTG, isopropyl β-D-thiogalactopyranoside; Tricine, *N*-tris(hydroxymethyl)methylglycine; TSP, sodium 3-(trimethylsilyl)propionate-*2,2,3,3-d*$_4$; NOE, nuclear Overhauser effect; NOESY, nuclear Overhauser effect spectroscopy; 19-NTHS, 19-nortestosterone hemisuccinate; TOCSY, total correlation spectroscopy.

of neutralized ammonium sulfate to about 30% saturation at 4 °C. The isomerase suspension was centrifuged and dissolved in appropriate buffers, and UV spectra and specific activity were obtained prior to use. Purified isomerase was stored as a crystalline suspension in 30% saturated and neutralized ammonium sulfate solution at 4 °C and was found to be stable for more than 1 year under these conditions. The preparations used for NMR studies had specific activities of 22 400 μmol min^{-1} (mg of protein)$^{-1}$, characteristic of the homogeneous enzyme. SDS−PAGE confirmed the enzyme to be ≥98% pure.

Preparation of NMR Samples. Enzyme concentrations were determined by using the absorbance at 280 nm (ϵ = 1890 M^{-1} cm^{-1}) for the native enzyme and at 293 nm (ϵ = 2390 M^{-1} cm^{-1}) for the ionized tyrosinate form at pH 13.0 (Goodwin & Morton, 1946). At subunit concentrations exceeding 1.0 mM, significant decreases in NMR signal intensities were observed, presumably due to the well-documented aggregation of isomerase at high concentrations (Benson et al., 1975). Therefore, concentrations of isomerase ≤0.75 mM with respect to subunits were used for NMR studies.

NMR samples were prepared in 10 mM sodium phosphate, 20 mM sodium chloride, 1.1 mM 19-NTHS (dissolved in DMSO-d_6), 9% (v/v) DMSO-d_6, pH 7.2, in H_2O or in D_2O. The pH values were determined in the presence of 9% (v/v) DMSO-d_6 at 20 °C and are uncorrected for the samples in D_2O.

NMR Spectroscopy. Unless otherwise noted, NMR experiments were performed on a Varian Unityplus 600 spectrometer equipped with four independent RF channels and *z*-gradient capabilities at 37 °C using the Nalorac 8 mm triple resonance, pulsed field gradient probe and with 2.2 cm sample columns (850 μL) in Shigemi 8 mm NMR tubes. All multidimensional data sets were recorded using the States−TPPI method (Marion et al., 1989) in all indirect dimensions, with a relaxation delay of 1.1 s. Table 1 summarizes the data acquisition and processing parameters for all of the NMR experiments recorded for the isomerase−19-NTHS complex. In some NMR experiments, the original pulse sequences were modified to include gradient pulses and water flip-back pulses in order to minimize artifacts and to avoid saturation of the water resonances (Table 1). As indicated, the data were collected using three protein samples, in which the protein is either uniformly labeled with ^{15}N and dissolved in H_2O or uniformly doubly labeled with ^{15}N and ^{13}C and dissolved in H_2O or D_2O. After prolonged NMR experiments at 37 °C, the enzyme retained more than 85% of its activity.

The sequence-specific backbone assignments were obtained with a minimum number of triple resonance 3D experiments, namely, HNCACB and HNCO, and were confirmed by sequential NOE data in three NOESY spectra (Table 1). The aliphatic side chain assignments were made mainly from ^{1}H−^{13}C CT-HSQC and 3D HCCH-TOCSY data. For aromatic side chain assignments, ^{1}H−^{13}C CT-HSQC and 3D ^{1}H−^{13}C NOESY-CT-HSQC experiments optimized for aromatic ^{1}H−^{13}C pairs were performed on a Varian 750 MHz Unityplus spectrometer, kindly made available to us by Prof. D. Gorenstein at the University of Texas, Medical Branch, Galveston, TX.

In addition, ^{1}H−^{15}N HSQC titrations with steroids (19-NTHS and doxyl-DHT) were carried out in a 5 mm triple resonance pulsed field gradient probe using standard 5 mm NMR tubes. The doxyl-DHT titration data were collected at 500 MHz using a Varian Unityplus 500 NMR spectrometer. At 37 °C, the water resonance (H_2O or HOD) is taken as 4.658 ppm downfield from TSP, and this chemical shift difference was used to match the probe temperatures of the three NMR spectrometers used.

All data sets were processed on Silicon Graphic workstations (Indigo^{2}XZ or Personal IRIS 4D/35) using the FELIX software package (Biosym Technologies). The observed ^{1}H chemical shifts are reported with respect to the H_2O or HOD signal, which is taken as 4.658 ppm downfield from external TSP at 37 °C. The carbon chemical shifts are reported with respect to external TSP in D_2O (0.0 ppm). The nitrogen chemical shifts are reported with respect to external [^{15}N]NH_4Cl (2.9 mM in 1 M HCl) at 20 °C, which is 24.93 ppm downfield from liquid NH_3 (Levy & Lichter, 1979).

Observation of Slowly Exchanging Amide Protons with Deuterons. Crystalline ^{15}N- and ^{13}C-labeled isomerase (10 mg), obtained by centrifugation from a saturated and neutralized ammonium sulfate slurry was equilibrated with 2.0 mL of 50% saturated deuterated ammonium sulfate in D_2O for 1 week at 4 °C to decrease the H_2O content of the enzyme crystals. After the supernatant fraction was carefully removed by centrifugation, the NH exchange with D_2O was initiated by dissolving the enzyme crystals in 850 μL of 10 mM sodium phosphate buffer with 20 mM NaCl and 9% (v/v) DMSO-d_6, pH* 7.25 (meter reading), in D_2O, and 1.1 mM 19-NTHS was introduced from a stock solution in DMSO-d_6. A series of ^{1}H−^{15}N HSQC spectra were then collected at 600 MHz. The first HSQC spectrum was started 2 h after the enzyme was dissolved in D_2O at 37 °C and was recorded with 128 complex points in t_1 and eight scans per FID for a total time of 1.1 h. Two more HSQC spectra were recorded starting at 7 h (16 scans per FID, total time 2.2 h) and at 82 h (96 scans per FID, total time 12.7 h).

^{1}H−^{15}N HSQC Titrations of Isomerase with Steroids. HSQC titrations of isomerase with 19-NTHS or with doxyl-DHT were carried out in 5 mm NMR tubes initially containing a volume of 600 μL. Isomerase (0.65 mM sites) was titrated with 19-NTHS at concentrations of 0, 91, 197, 349, 636, 923, 1210, and 1497 μM added from 5.6 or 184 mM stock solutions of 19-NTHS in DMSO-d_6, monitoring the ^{1}H−^{15}N HSQC spectra at 600 MHz. The shift of each ^{1}H−^{15}N correlation peak was monitored during the titration using an in-house computer program. The amide correlations were assigned in the free enzyme by tracking the peak positions from the isomerase−19-NTHS complex. The ^{15}N and NH chemical shifts of free and steroid-bound isomerase are given in Table S2 of the Supporting Information.

Titrations with doxyl-DHT were carried out at 500 MHz with a Varian Unityplus 500 Varian NMR spectrometer because of the greater paramagnetic effects at lower field (Mildvan & Gupta, 1978). A series of ^{1}H−^{15}N HSQC spectra of 0.50 mM isomerase were recorded with increasing concentrations of doxyl-DHT (0, 1, 4, 10, 21, 33, 47, 62, 91, 148, and 250 μM). Small volumes (1−2 μL) of doxyl-DHT stock solutions (0.33, 1.0, and 10 mM) were added to 660 μL of isomerase solution with a final dilution factor of isomerase less than 5%. At the end of the titration, 2 μL of 200 mM sodium ascorbate solution was added to the solution to provide a final concentration of 570 μM ascorbate. After 15 min at 37 °C, another ^{1}H−^{15}N HSQC spectrum was recorded. The volumes of individual cross peaks in different HSQC spectra were measured using the peak-picking func-

Table 1: Data Acquisition and Processing Parameters of All NMR Experiments

no.	experiment	pulse sequence ref	isotope labeling	dimension	sweep width (Hz)	center (ppm)	acq time (ms)	no. of complex points	mixing time (ms)	nt	total time (h)	data matrix real points	digital res. (ppm/pt)
1.	2D ^{1}H−^{15}N HSQC	*a*	^{15}N	^{15}N (t_1)	1740	119.00	147.1	256		4	1.1	1024	0.03
				NH (t_2)	10000	4.66	128.0	1280				1024	0.004
2.	3D ^{1}H−^{15}N TOCSY-HSQC	*b*	^{15}N	^{1}H (t_1)	7200	4.66	8.9	64	22.5	16	50	512	0.023
				^{15}N (t_2)	1740	119.00	18.4	32				128	0.22
				NH (t_3)	10000	4.66	64.0	640				512	0.008
3.	3D ^{1}H−^{15}N NOESY-HSQC	*c*	^{15}N	^{1}H (t_1)	7200	4.66	14.4	104	100	16	83	512	0.023
				^{15}N (t_2)	1740	119.00	18.4	32				128	0.22
				NH (t_3)	8000	4.66	64.0	512				512	0.008
4.	3D ^{1}H−^{15}N HMQC-NOESY-HSQC	*d*	^{15}N	^{15}N (t_1)	1740	119.00	18.4	32	100	16	24	128	0.22
				^{15}N (t_2)	1740	119.00	18.4	32				128	0.22
				NH (t_3)	10000	4.66	64.0	640				512	0.008
5.	2D ^{1}H−^{13}C CT-HSQC	*e*	^{15}N/^{13}C	^{13}C (t_1)	9052	43.00	23.0	208		64	12	1024	0.015
				^{1}H (t_2)	8800	2.60	58.0	512				2048	0.004
6.	3D HNCO	*f*	^{15}N/^{13}C	^{13}C (t_1)	1810	175.00	23.2	42		8	17	256	0.05
				^{15}N (t_2)	1740	119.00	18.4	32				128	0.22
				NH (t_3)	10000	4.66	64.0	640				512	0.008
7.	3D HNCACB	*g*	^{15}N/^{13}C	^{13}C (t_1)	9052	43.00	5.3	48		32	75	512	0.12
				^{15}N (t_2)	1740	119.00	18.4	32				128	0.22
				NH (t_3)	10000	4.66	64.0	640				512	0.008
8.	3D HCCH−TOCSY	*h*	^{15}N/^{13}C	^{1}H (t_1)	4400	2.60	20.9	92	17.8	16	72	512	0.014
				^{13}C (t_2)	4525	43.00	7.1	32				128	0.23
				^{1}H (t_3)	8800	2.60	58.0	512				512	0.014
9.	3D ^{1}H−^{13}C HMQC-NOESY-HSQC	*d*	^{15}N/^{13}C	^{13}C (t_1)	9048	43.00	10.2	92	150	16	72	512	0.12
				^{15}N (t_2)	1740	119.00	18.4	32				128	0.22
				NH (t_3)	8000	4.66	64.0	512				512	0.008
10a.	2D ^{1}H−^{13}C NOESY-HSQC	*i*	^{15}N/^{13}C	^{1}H (t_1)	7500	4.66	17.1	128	150	128	15	1024	0.012
				^{1}H (t_2)	8400	4.66	61.0	512				1024	0.007
				^{13}C		43.00							
10b.	3D ^{1}H−^{13}C NOESY-HSQC	*i*	^{15}N/^{13}C in D_2O	^{1}H (t_1)	7500	4.66	12.3	92	100	16	72	512	0.024
				^{13}C (t_2)	4525	43.00	7.1	32				128	0.23
				^{1}H (t_3)	8400	4.66	61.0	512				512	0.014
11.	2D [^{1}H−^{13}C]$_{aromatic}$ CT-HSQC[l]	*e*	^{15}N/^{13}C in D_2O	^{13}C (t_1)	1980	130.00	16.2	32		128	4	256	0.04
				^{1}H (t_2)	8000	4.66	64.0	512				512	0.006
12.	3D [^{1}H−^{13}C]$_{aromatic}$ NOESY CT-HSQC[l]	*j*	^{15}N/^{13}C in D_2O	^{1}H (t_1)	6900	4.06	9.3	64	100	32	63	256	0.036
				^{13}C (t_2)	1980	130.00	12.1	24				64	0.16
				^{1}H (t_3)	8000	4.66	64.0	512				256	0.010
13a.	2D [^{1}H−^{13}C]$_{aliphatic}$ HMQC-NOESY	*k*	^{15}N/^{13}C in D_2O	^{1}H (t_1)	6000	4.66	21.3	128	350	128	13	512	0.02
				^{13}C		43.00							
				^{1}H (t_2)	8000	4.66	128.0	1024				1024	0.007
13b.	2D [^{1}H−^{13}C]$_{aliphatic}$ HMQC-NOESY	*k*	^{15}N/^{13}C in D_2O	^{13}C (t_1)	9050	43.00	14.1	128	350	128	13	512	0.12
				^{1}H (t_2)	8000	4.66	128.0	1024				1024	0.007
13c.	2D [^{1}H−^{13}C]$_{aromatic}$ HMQC-NOESY	*k*	^{15}N/^{13}C in D_2O	^{1}H (t_1)	5400	4.66	23.7	128	350	160	16	512	0.018
				^{13}C		130.00							
				^{1}H (t_2)	8000	4.66	128.0	1024				1024	0.007
13d.	3D [^{1}H−^{13}C]$_{aliphatic}$ HMQC-NOESY	*k*	^{15}N/^{13}C in D_2O	^{1}H (t_1)	1320	1.10	24.2	32	350	32	60	256	0.01
				^{13}C (t_2)	3016	20.0	10.6	32				128	0.16
				^{1}H (t_3)	8000	4.66	64.0	512				256	0.01

[a] Bodenhausen & Ruben, 1980; Mori et al., 1995. [b] Marion et al., 1989; Zang et al., 1994. [c] Marion et al., 1989; Abeygunawardana et al., 1996. [d] Ikura et al., 1990; Kay et al., 1990a; modified to incorporate water flip-back HSQC sequence of Mori et al. (1995). [e] Vuister & Bax, 1992. [f] Kay et al., 1990b, 1994. [g] Wittekind & Muller, 1993; Muhandirum & Kay, 1994. [h] Bax et al., 1990; Kay et al., 1993. [i] Marion et al., 1989; Pascal et al., 1994. [j] HSQC module of the NOESY-HSQC sequence (i) was replaced by CT-HSQC to improve resolution. [k] Lee et al., 1994. [l] Acquired at 750 MHz.

tion of Felix 2.3 (Biosym Technologies), and the data were analyzed with an in-house computer program to yield [doxyl-DHT]$_{50}$, the concentration of spin-label which halved the signal volume for each residue.

EPR and Water Proton Relaxation by Doxyl-DHT. The paramagnetic contributions to the longitudinal relaxation rates ($1/T_{1p}$) of water protons were obtained at 24.3 MHz (Mildvan & Engle, 1972) with 100 and 200 μM doxyl-DHT in water containing 9.0% (v/v) DMSO-d_6 by the pulsed method with an NMR Specialties PS 60-W NMR spectrometer. EPR spectra of 40 μL aliquots of doxyl-DHT solutions (100 and 200 μM) were measured in quartz capillary tubes fitted with Teflon plugs in a Varian E-4 EPR spectrometer (Mildvan & Engle, 1972).

Intermolecular NOEs between Isomerase and 19-NTHS. A solution (0.85 mL) containing 0.75 mM uniformly ^{13}C- and ^{15}N-labeled isomerase, 6.0 mM 19-NTHS, 10 mM sodium phosphate buffer, pH 7.2, 20 mM NaCl, and 9% (v/v) DMSO-d_6 in D_2O was placed in an 8 mm Shigemi tube and equilibrated at 37.0 °C in the Nalorac 8 mm probe for $\geq$20 min. 2D and 3D ^{13}C-filtered isotope-edited NOESY spectra (Lee et al., 1994) were collected as described in Table 1. A long mixing time of 350 ms was used to optimize the intermolecular NOE's in this fast exchanging system, as is generally found to be necessary (Lee et al., 1995).

RESULTS

^{1}H−^{15}N HSQC Spectra of Isomerase. ^{1}H−^{15}N HSQC spectra of free isomerase and its 19-NTHS complex are shown in Figure 2. Only one set of signals is seen, indicating a symmetric dimer, in both the free and bound state. Line widths of the cross peaks in the HSQC spectra are consistent with a dimer of molecular mass 27 kDa. The correlation time for the Y55F/Y88F mutant was 18 ns as measured by

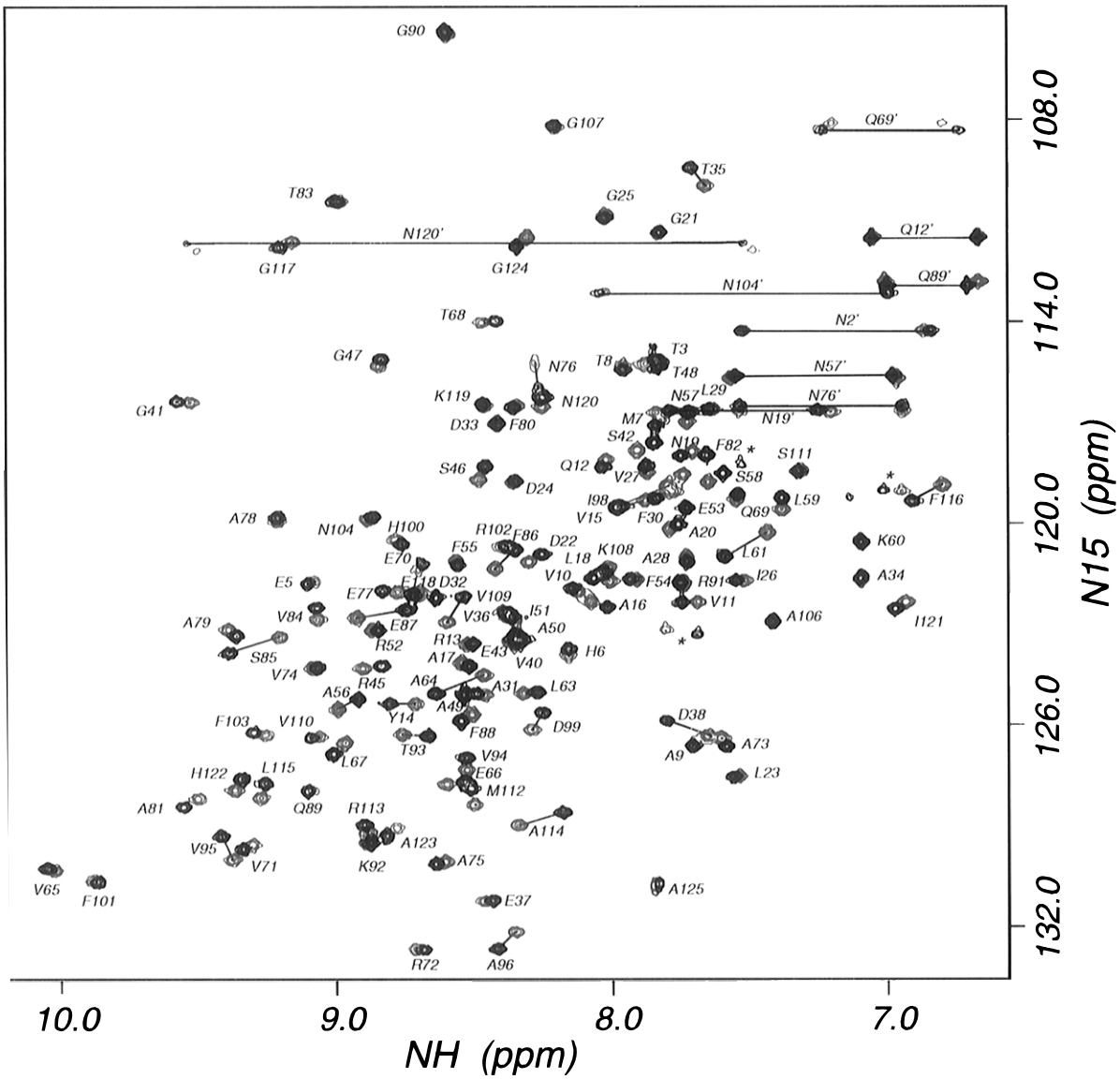

FIGURE 2: $^{1}H-^{15}N$ HSQC spectra of free and 19-NTHS-bound isomerase. The resonances of the free enzyme are shown in red, and those of 19-NTHS-bound isomerase are in black. The horizontal lines indicate amide side chain resonances. Where necessary, red lines connect the signal of the free enzyme with the corresponding signal of the complex.

^{13}C NMR relaxation studies of side chain and backbone resonances of Tyr-14 (Zhao et al., 1996a) and independently by time-resolved fluorescence spectroscopy (Wu et al., 1994). Changes in ^{15}N and NH chemical shifts upon the binding of the steroid are detected such that the 135 cross peaks present in the $^{1}H-^{15}N$ HSQC spectra are slightly more dispersed in the complex (shown in black) than in the free enzyme (shown in red). These cross peaks account for 117 of the 119 backbone amides and all of the nine pairs of side chain amides (six asparagine and three glutamine residues), taking into account Met-1 and the five proline residues in the amino acid sequence. The peaks for Asn-2 and Gly-105 are not observed in the $^{1}H-^{15}N$ HSQC spectra, presumably due to fast exchange with water. The amide ^{15}N and NH resonances of the complex were assigned on the basis of the heteronuclear triple resonance experiments discussed below, whereas those of the free enzyme were assigned by following the peak movements in the HSQC titrations with increasing concentrations of 19-NTHS.

Resonance Assignments. Sequence-specific backbone resonance assignments were obtained primarily by 3D HNCACB spectra (Table 1, Figure 3). In these experiments, each backbone NH shows correlation peaks to its own Cα and Cβ resonances as well as to the Cα and Cβ resonances of the preceding residue. In general, correlations with the preceding residue show lower peak intensities than those of the intraresidue correlations. Stretches of NH resonances were then aligned by matching each of the [Cα and Cβ]$_{i-1}$ interresidue chemical shifts to one with [Cα and Cβ]$_i$ intraresidue chemical shifts. Sequence-specific alignments of short stretches were then obtained by the use of the characteristic chemical shifts of the Cα of 9 glycines, Cα of 5 prolines, and the Cβ of 21 alanines, 5 serines, and 7 threonines as starting points (Grzesiek & Bax, 1993). In isomerase these residues were well dispersed throughout the amino acid sequence, yielding nearly complete sequence-specific assignments. These data, together with Hα assignments from 3D $^{1}H-^{15}N$ TOCSY-HSQC spectra, accurate Hα and Cα assignments from $^{1}H-^{13}C$ CT-HSQC spectra, and carbonyl assignments from 3D HNCO spectra completed the sequence-specific backbone assigments. In addition, sequential (i, $i + 1$) NH to NH, Hα to NH, and Hβ to NH NOE correlations observed in 3D $^{1}H-^{15}N$ NOESY-HSQC spectra (Figure 4) confirmed most of the backbone resonance assignments.

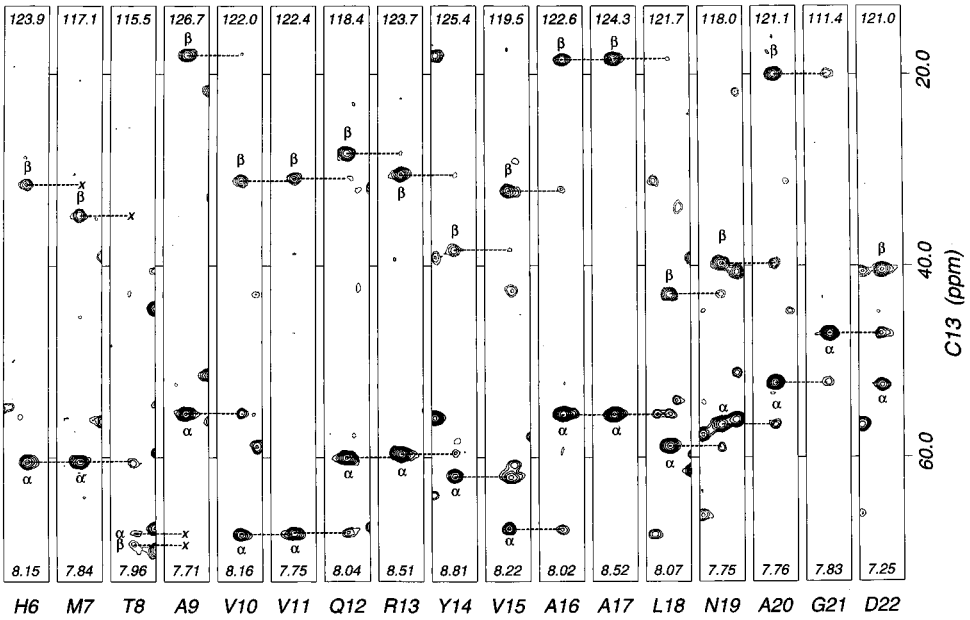

FIGURE 3: Sequential strips from the 3D HNCACB experiment for residues His-6 to Asp-22 (helix 1) of the isomerase−19-NTHS complex. Each strip represents a 2D plane taken at the indicated ^{15}N chemical shift (upper) and a 0.25 ppm window centered at the NH chemical shift of each residue (lower). The Cβ contours (dotted) are negative. The horizontal lines show sequential through-bond connectivities. The x's indicate cross peaks seen at lower contour levels.

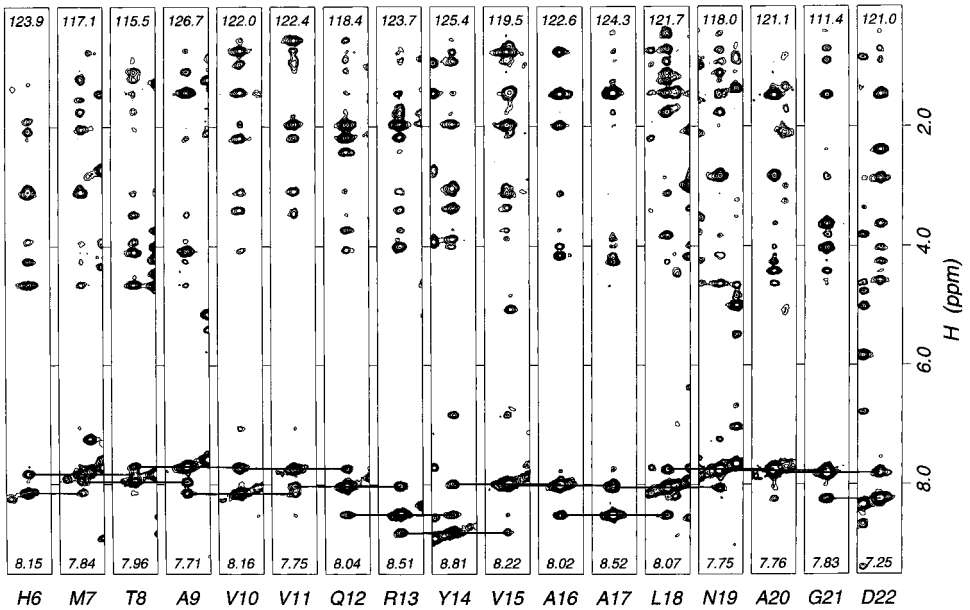

FIGURE 4: Sequential strips from the 3D ^{1}H−^{15}N NOESY-HSQC spectrum of the isomerase−19-NTHS complex (t_{mix} = 100 ms) showing the residues of helix 1. Each strip represents a 2D plane taken at the indicated ^{15}N chemical shift (upper) and a 0.25 ppm window centered at the NH chemical shift of each residue (lower). The horizontal lines show sequential NH to NH NOE connectivities.

Side chain assignments were made primarily from 3D HCCH-TOCSY spectra. Starting from Cα−Hα correlations, these experiments yielded complete carbon and proton resonance assignments of all aliphatic side chains with the exception of Arg-52, Arg-72, Pro-97, and Arg-113. HCCH-TOCSY data also yielded Cβ and Hβ assignments of all of the aromatic residues (Table S1). Side chain amide resonances of Glu and Asn residues in ^{1}H−^{15}N HSQC spectra were sequence specifically assigned by intraresidue NOE connectivities in 3D ^{1}H−^{15}N NOESY-HSQC spectra. The complete resonance assignments of isomerase complexed with 19-NTHS are given in Table S1 of the Supporting Information.

Secondary Structure. The secondary structure of isomerase complexed with 19-NTHS was derived from both ^{1}H and ^{13}C chemical shift indices and NOE measurements. *(a) Chemical shift indices.* The chemical shift differences of the Hα, Cα, Cβ, and CO resonances from their random coil values are shown in Figure 5. The consensus chemical shift indices were derived from these four sets of data (Wishart et al., 1992; Wishart & Sykes, 1994) and are shown in Figure 6. Individual sets of chemical shift indices for the Hα, Cα, Cβ, and CO resonances are provided in Figure S1 of the Supporting Information. The secondary structure of isomerase was assigned on the basis of the chemical shift indices which are independent of the dimeric structure of this enzyme. *(b) Interresidue NOE's.* Sequential and near neighbor interproton NOE's, initially assumed to be intramonomeric, were used independently to derive the secondary structure (Figure 6). The close agreement in secondary structure obtained by these two methods supports this assumption.

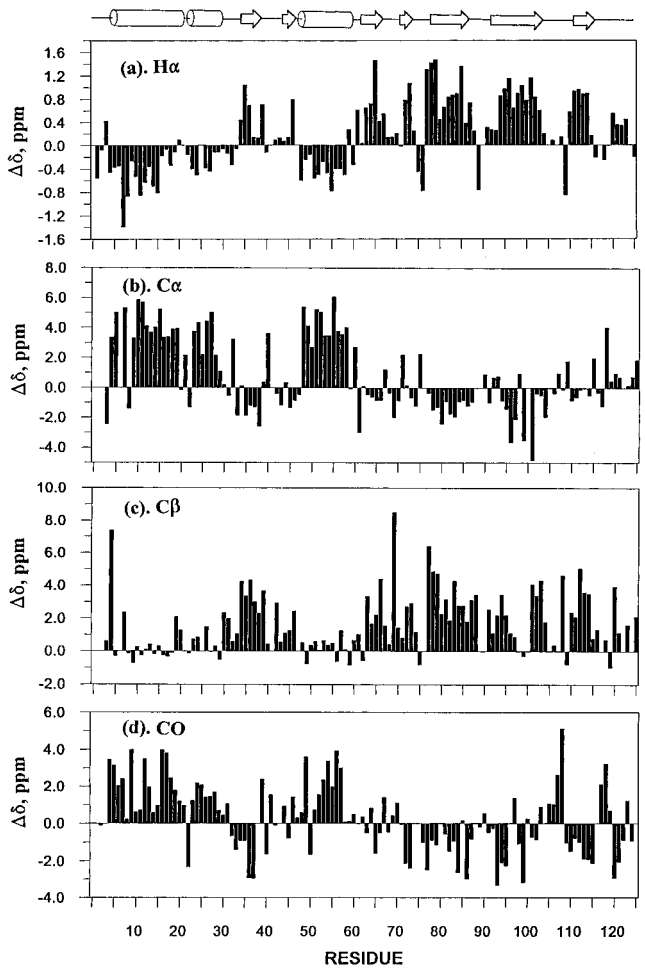

FIGURE 5: Backbone chemical shift differences from those for random coils for each residue of isomerase complexed with 19-NTHS. The standard values for Hα were from Wishart et al. (1992), for CO were from Wishart and Sykes (1994), and for Cα and Cβ were from Spera and Bax (1991).

Helices. Helical regions were identified on the basis of three criteria: (1) a series of continuing upfield-shifted Hα and Cβ resonances (Spera & Bax, 1991; Wishart et al., 1992; Wishart & Sykes, 1994) and downfield-shifted Cα and CO resonances (Wishart et al., 1991; Wishart & Sykes, 1994), (2) strong NN (*i, i + 1*) NOE's, weak or absent αN (*i, i + 1*) NOE's, and the presence (for an α-helix) or the absence (for a 3_{10} helix) of the αN (*i, i + 4*) NOE's, and (3) slow amide hydrogen exchange patterns (Wüthrich, 1986). On the basis of these criteria, residues 5−21 (helix 1) and residues 48−60 (helix 3) were identified as α-helices, whereas residues 23−30 (helix 2) possibly formed a short 3_{10} helix as indicated by absent or very weak αN (*i, i + 4*) NOE's and the presence of αN (*i, i + 2*) NOE's (Figure 6). Steroid-bound isomerase thus contains a total of 38 out of 125 residues (30%) in helices. Helix 1 contains the catalytic general acid, Tyr-14, which donates a hydrogen bond to the 3-carbonyl group of 19-NTHS hemisuccinate (Kuliopulos et al., 1991).

β-Structure. β-Strands were identified by three criteria: (1) sequential and continuous downfield-shifted Hα and Cβ resonances (Spera & Bax, 1991; Wishart et al., 1992; Wishart & Sykes, 1994) and upfield-shifted Cα and CO resonances (Wishart et al., 1991), (2) strong αN (*i, i + 1*) NOE's, and weak or absent NN (*i, i + 1*) NOE's, and (3) slow amide hydrogen exchange patterns (Wüthrich, 1986). Assuming all interactions to be intrasubunit, one β-hairpin[2] and an extensive β-sheet near the C-terminus were identified (Figures 5−7). All β-strand interactions in isomerase were found to be antiparallel on the basis of remote NOE's, with the exception of a parallel interaction between β1 and β7 which may be intersubunit (Figure 7).

The β-hairpin, which contains the catalytic base Asp-38, consists of the β1 strand (residues 34−38) and the β2 strand (residues 44−47) closed by a nonclassical β-turn (residues 39−42) (Figure 7A). The β-hairpin shows slow NH exchange in its antiparallel region but fast exchange near the β-turn (Figure 6). Pro-39, the first residue of this β-turn, is in a *cis* conformation, based on the four criteria of Wüthrich (1986), namely, the presence of $H\alpha-H\alpha_{i-1}$ and $H\alpha-NH\alpha_{i-1}$ NOE's and the absence of $H\delta_2-H\alpha_{i-1}$ and $H\delta_2-NH_{i-1}$ NOE's. The other four prolines of isomerase are *trans*, based on all four criteria (Pro-4) or on two criteria, the presence of $H\delta_2-H\alpha_{i-1}$ and the absence of $H\alpha-H\alpha_{i-1}$ NOE's (Pro-44, 62, and 97).

The large C-terminal β-sheet contains four antiparallel strands, the first strand of which consists of β3 and β4 (residues 62−67, 71−73), interrupted by a bulge or loop between residues 68 and 70 (Figure 7B). The first and second strands (β5, residues 78−87) of this sheet are connected by a nonclassical turn, the second and third strands (β6, residues 92−104) are connected by a type II β-turn, and the third and fourth strands (β7, residues 111−116) are connected by a loop containing an apparent type I β-turn (residues 105−108). Another apparent type I β-turn is found between residues 119 and 122 near the C-terminus. The presence and types of β-turns are based solely on NOE criteria. Thus, β-strands constitute 47 residues (38%) and turns constitute 20 residues (16%) of the structure of steroid-bound isomerase. The remaining 20 residues are assumed to be in coils, constituting 16% of the structure. Figure 8A summarizes the secondary structure of isomerase, making the simplest assumption that all near-neighbor NOE's are intrasubunit.

HSQC Titrations with 19-NTHS. 19-NTHS, a product analog and substrate of the reverse isomerase reaction, is a linear competitive inhibitor of isomerase with a K_i of 10 μM under the present conditions (Zhao et al., 1996a). HSQC titrations revealed that 42 resonances of isomerase showed significant changes in ^{15}N, and 40 resonances showed significant changes in NH chemical shifts on binding 19-NTHS. The chemical shift changes of the backbone ^{15}N and NH resonances of isomerase (0.65 mM) induced by the binding of 19-NTHS (1.2 mM) are summarized in Figures 8B and 9 and are given in detail in Table S2 of the Supporting Information. Figure 9 shows the NH (Figure 9a) and ^{15}N (Figure 9b) chemical shift changes induced by ligand binding in the 1:1 complex. The weighted sum of the chemical shift changes of both nuclei for all residues (Figure 9c) was calculated on the basis of the spectral dispersion at these two dimensions and plotted with respect to residue number, indicating the overall effects on each individual amide NH group. Sharp end points in the HSQC titrations were observed at 1:1 stoichiometry, consistent with tight

[2] While an *intrasubunit* β-hairpin provides the simplest explanation of the NOE's between the β1 and β2 strands, an alternative explanation which cannot be excluded is an *intersubunit* antiparallel interaction between the β1 and β2 strands with the bulging out of residues 40−43 from both strands.

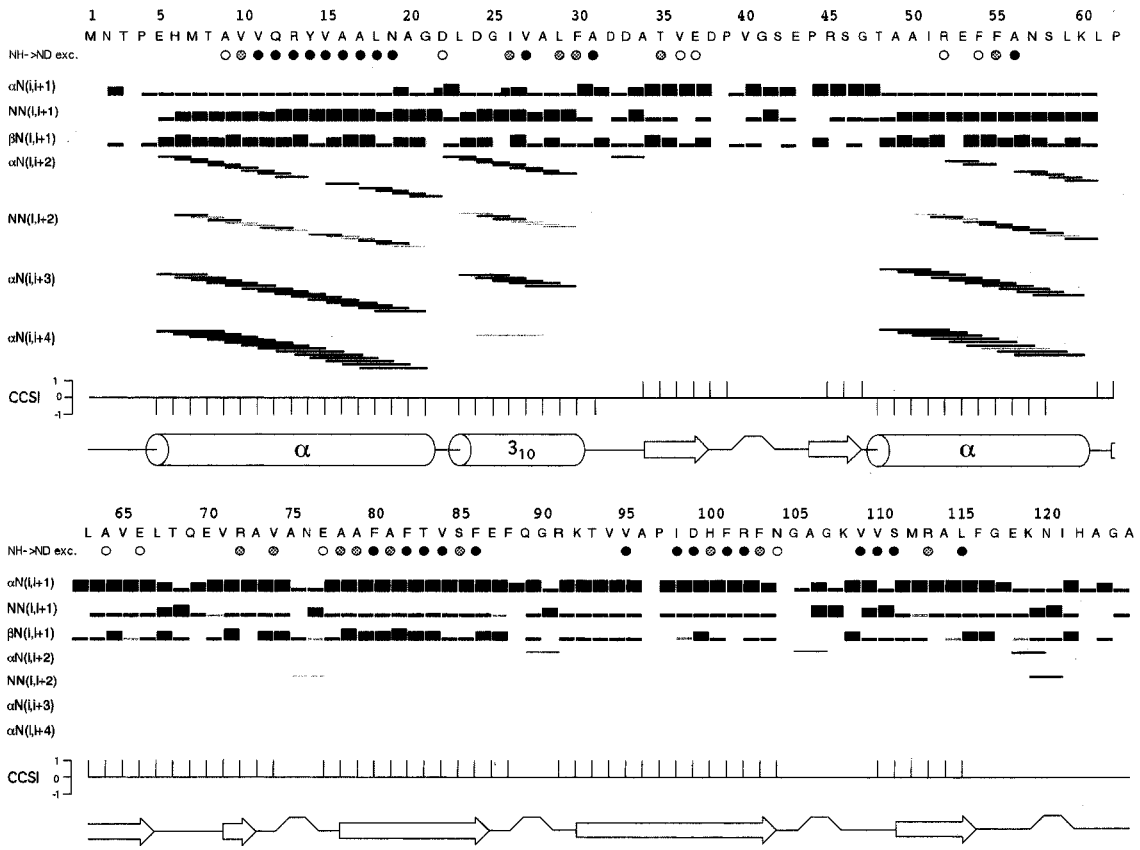

FIGURE 6: Diagram summarizing near-neighbor NOE's and the secondary structure of isomerase complexed with 19-NTHS. Slowly exchanging amide protons at 37 °C are indicated by open circles (2.5 h < t < 8.1 h), shaded circles (8.1 h < t < 88.4 h), and filled circles (t > 88.4 h). The consensus chemical shift indices (CCSI) of the Hα, Cα, Cβ, and CO (Wishart et al., 1992; Wishart & Sykes, 1994) are shown in the bottom panel. The gray shading indicates ambiguous NOE's due to overlapping resonances.

binding at the active site (Figure 10). Beyond 1:1 stoichiometry, four resonances showed very small further changes in chemical shifts, presumably due to very weak, nonspecific steroid binding.[3]

Significant changes in backbone NH chemical shifts on steroid binding occurred near Tyr-14 in helix 1, at the carboxyl half of helix 3, at the end of the 3_{10} helix, throughout the β-hairpin, and along β-strands 3, 5, 6, and 7 of the large antiparallel β-sheet (Figure 8B), suggesting that these regions contribute to the substrate binding site. Helix 1 contains Tyr-14, the general acid catalyst, and the β-hairpin contains Asp-38, the general base. No significant effects of steroid binding were observed on the chemical shifts of the nine pairs of resonances of the side chain amide groups of asparagine and glutamine residues.

Intermolecular NOE's from isomerase to 19-NTHS. In 2D and 3D ^{13}C-filtered isotope-edited NOESY studies of the complex of 19-NTHS with ^{13}C-labeled isomerase in D_2O (data not shown), numerous NOE's from the ^{13}C-bound protons of the enzyme to the ^{12}C-bound protons of the steroid were detected (Table 2, Figures 8C and 11A). Because of the previously reported isomerase-catalyzed deuteration at the 2α-, 2β-, 4-, 6α-, and 6β-positions of 19-NTHS in D_2O (Kuliopulos et al., 1991), NOE's to these protons were not detected in the present work. However, previous NOESY studies in H_2O have established the presence of NOEs from the Tyr-14 ϵ-protons to the 2α- and 2β-protons of 19-NTHS (Kuliopulos et al., 1991). These NOE's, together with those that were unequivocally assigned in the present work, based on both ^{13}C and ^{1}H chemical shifts (Table 2, Figure 11A), indicate that the A ring of the bound steroid is near Tyr- 14 and Leu-18 of helix 1 and Leu-59 of helix 3. The B ring is near Leu-18 of helix 1, Leu-63 of β-strand 3, and Val-84 of β-strand 5. The C ring is near Leu-59 of helix 3, Leu-61 and Leu- 63 of β-strand 3, Val-84 of β-strand 5, and Val-95 of β-strand 6 of the antiparallel β-sheet. The D ring is near Val-84 and Phe-86 of β-strand 5 and Thr-93 and Val-95 of β-strand 6. The succinate methylene protons are near Leu-18 of helix 1, Leu-61 and Phe-86 of β-strand 5, Phe-88 of the adjacent type II β-turn, Met-112 and Ala-114 of β-strand 7, and Ile-121 of the last β-turn. Most of the proximities of the steroid to the antiparallel β-sheet formed from β-strands 3−7 are near one end of the hydrophobic face of the β-sheet, centered near Val-84, Phe-86, Thr-93, and Val-95 (Figure 8C).

Figure 11A summarizes the proximal residues and Figure 8C summarizes the regions of the isomerase secondary structure that are near the bound steroid on the basis of intermolecular NOE's. These regions correlate with regions that showed changes in ^{15}N and NH chemical shifts which are summarized in Figure 8B. To satisfy all of the observed proximities between 19-NTHS and isomerase simultaneously, the enzyme must fold to place helices 1 and 3 near the

[3] The residues affected by weak nonspecific binding of the steroid beyond 1:1 stoichiometry are Asp-38, Phe-82, Ser-85, and Ala-114. Such weak, nonspecific steroid binding sites have previously been detected with 5α-estrane-3,17-dione, a UV transparent steroid which selectively narrows the UV absorption bands of Tyr-14 with a sharp end point at 1:1 stoichiometry, beyond which the UV absorbancies of Tyr-14 and of several phenylalanine residues increase slightly with steroid concentration (Zhao et al., 1995b). Because of the limited solubility of the steroid substrate, effects on catalytic activity of occupancy of these weak sites by substrate could not be tested kinetically.

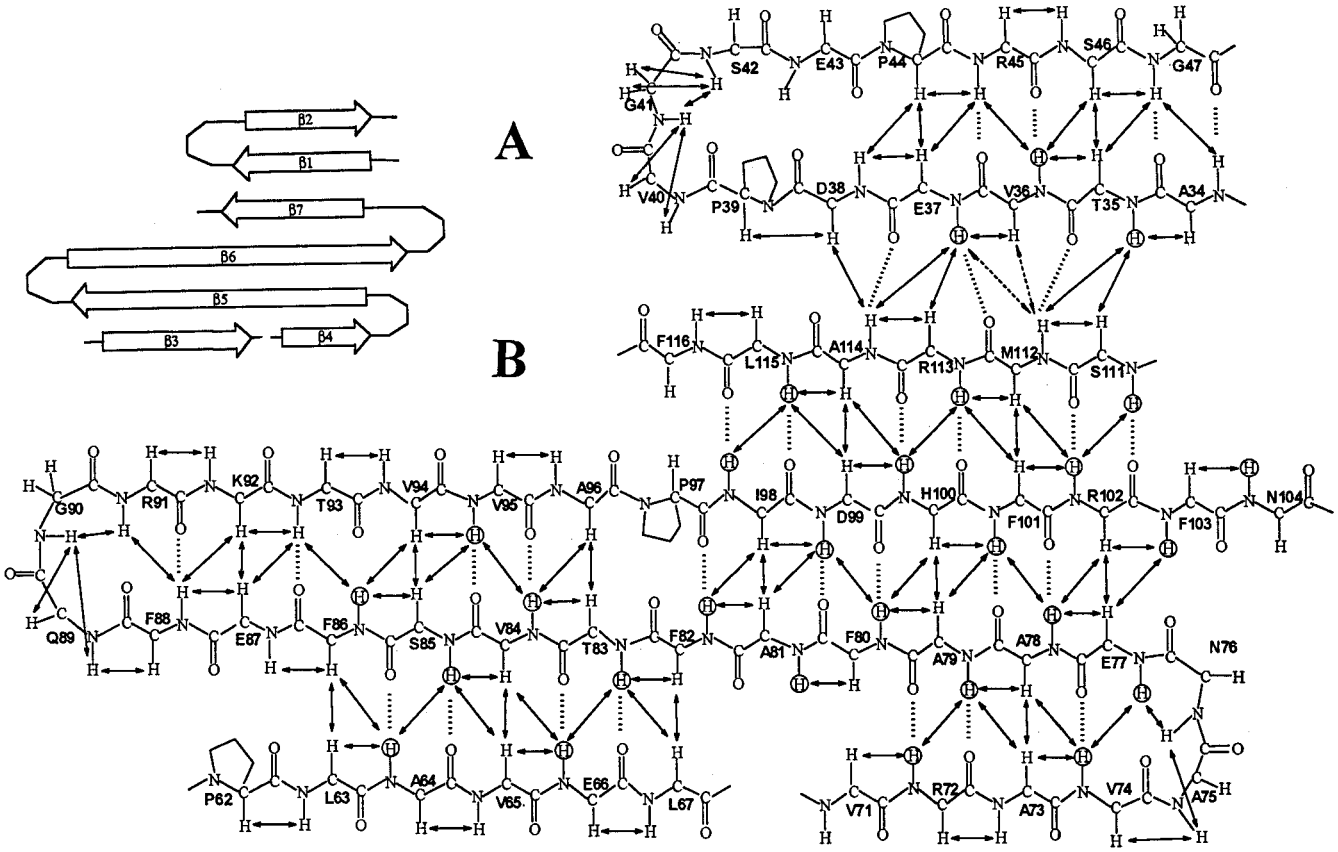

FIGURE 7: Diagram of the β-sheet structures of isomerase in its complex with 19-NTHS, assuming all interactions to be intrasubunit. (A) Structure of the β-hairpin. (B) Structure of the four-stranded antiparallel β-sheet. The parallel interaction between the β-hairpin and the β-sheet may be intersubunit.[2] Note that there are seven phenylalanine, four valine, two leucine, and three alanine residues on the same face of the β-sheet. Slowly exchanging amide protons are circled. Dashed, double-headed arrows indicate ambiguous NOE's due to overlapping resonances.

hydrophobic face of the β-sheet, thereby forming two walls of the active site. Whether this interaction is intra- or intersubunit is not known. The simultaneous proximity of Leu-61, Leu-63, Phe-86, and Val-95 to protons of both the α- and β-faces of the steroid (Table 2, Figure 11A) indicates that 19-NTHS binds to the active site of isomerase in either of two opposite orientations of its α- and β-faces. Such dual binding modes have previously been proposed to explain proton exchange with solvent from both faces of the steroid[4] (Schwab & Henderson, 1990; Kuliopulos et al., 1991; Viger et al., 1981).

HSQC Titrations with a Paramagnetic Substrate Analog. The spin-labeled steroid doxyl-DHT (Figure 1), a competitive inhibitor of isomerase with a K_i value of 25 μM, is known to bind exclusively to the active site of the enzyme with the nitroxide spin moiety oriented toward the solvent (Kuliopulos et al., 1987b). Hence the groups nearest the spin-label would be at, and just beyond, the D ring of a steroid substrate when bound in its proper orientation for catalysis. Prior to the HSQC titrations, the paramagnetic effect of free doxyl-DHT on $1/T_1$ of water protons, expressed as the molar relaxivity, was found to be 150 ± 40 M^{-1} s^{-1}, consistent with the reported value (140 ± 20 M^{-1} s^{-1}; Kuliopulos et al., 1987b).

The intensities of the backbone and nine side chain amide cross peaks in the $^1H-^{15}N$ HSQC spectra of 500 μM isomerase, as measured by cross peak volumes, were determined as a function of doxyl-DHT concentration over the range 0−250 μM. The paramagnetic effects of the spin-label on the HSQC spectra, under conditions of fast exchange, are dominated by dipolar effects on $1/T_2$ resulting in a decrease in cross peak intensity. These dipolar effects are inversely related to the sixth power of the distance ($1/r^6$) between each amide NH group and the nitroxide radical of the bound steroid (Mildvan & Gupta, 1978). Fast exchange of doxyl-DHT among many enzyme molecules was established by the complete disappearance of NH cross peaks of the most sensitive residues (58−61) at levels of the spin-label (33 μM) substoichiometric with the protein (500 μM), indicating that residues 58−61 at the end of helix 3 are closest to the bound nitroxide radical. Other NH signals disappeared at higher substoichiometric levels of doxyl-DHT due to their greater distance from the bound spin-label. That these losses in signal intensity were indeed due to paramagnetic effects was shown at the end of the HSQC titration by reducing the nitroxide with a 2.3-fold excess of ascorbic acid which restored the cross peaks to their original intensities, within experimental error.

The intensities of all paramagnetically affected NH cross peaks initially decreased linearly with doxyl-DHT concentration, permitting the titration data to be analyzed by using the initial points to extrapolate to the concentration of doxyl-

[4] NOE's to the methylene protons of the succinyl group from both remote edges of the β-sheet are found from the ϵ-methyl of Met-112 and the β-methyl of Ala-114 of β-strand 7 (weak) and from the δ-methyls 1 and 2 of Leu-61 near the beginning of β-strand 3 (medium). Also, NOE's from the δ-methyl 1 of Leu-18 to protons at both ends of the steroid are found, i.e., to 1β and/or 10β (medium) in ring A and to the 18-methyl and the succinate methylene protons (weak) near ring D. These remote effects may result from spin diffusion, from steroid interactions with residues from both subunits, from nonspecific second-site binding of 19-NTHS, or from a minor contribution from backward binding of 19-NTHS in the active site.

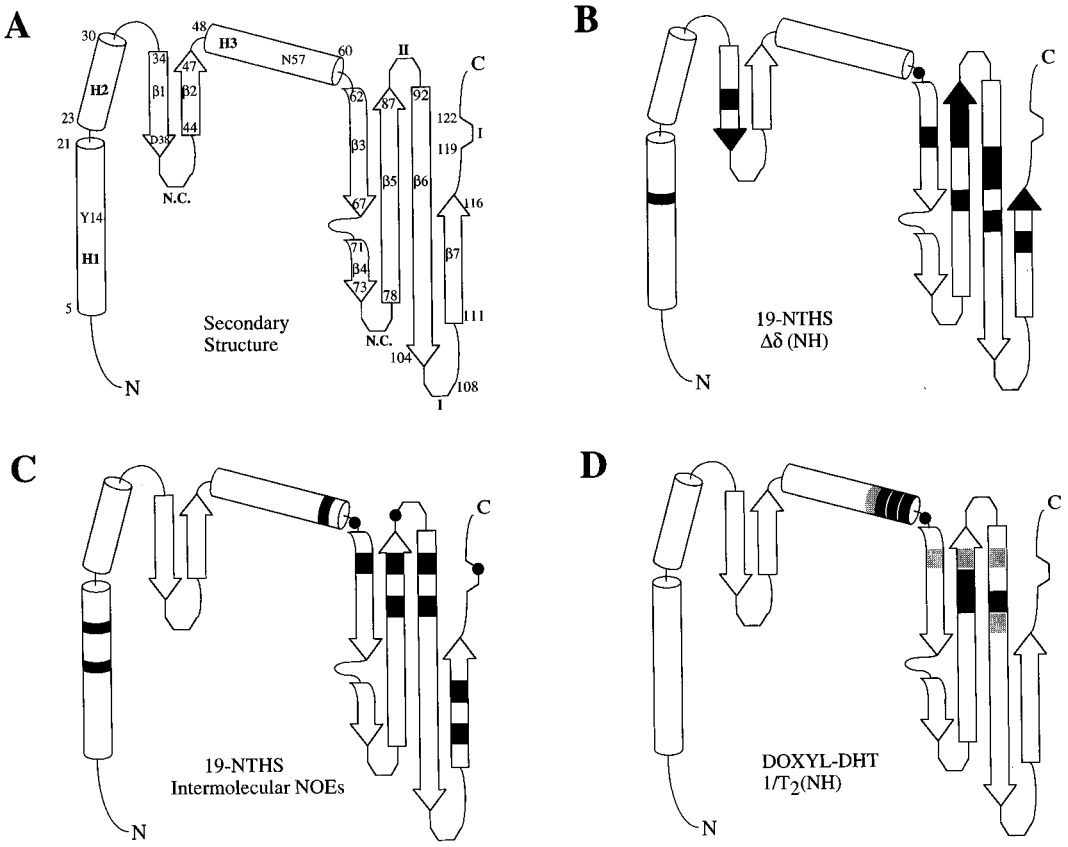

FIGURE 8: Diagram of the secondary structure and steroid binding site of Δ^5-3-ketosteroid isomerase. (A) Secondary structure assuming that all sequential and near-neighbor NOE's are intrasubunit as discussed in the text. The β1 strand forms a parallel interaction with β7, which may be intersubunit. Beginning and end points of secondary structural elements and locations of the active site residues Tyr-14, Asp-38, and Asn-57 are indicated. The types of turns are designated. N.C. refers to a nonclassical turn. (B) Regions of isomerase that show changes in the weighted sum of backbone ^{15}N and NH chemical shifts $\geq$0.1 ppm on binding 19-NTHS. (C) Regions of isomerase that show intermolecular NOE's from methyl and aromatic protons of the enzyme to protons of 19-NTHS. (D) Regions of isomerase that show very strong (black) or strong (gray) paramagnetic relaxation of backbone ^{15}N and NH resonances by the spin-labeled steroid, doxyl-DHT.

DHT required to halve the intensity of each attenuated cross peak, designated as [doxyl-DHT]$_{50}$. This value, when corrected by multiplication by the initial relative intensity of each affected cross peak, to ensure equal paramagnetic effects on transverse relaxation rates ($1/T_{2p}$) for each affected NH cross peak, yielded [doxyl-DHT]$_{50}^{corr}$. This corrected value is proportional to r^6, the (distance)^6 between the nitroxide and the NH group, as may be shown from the dipolar term of the Solomon−Bloembergen equation (Mildvan & Gupta, 1978):

$$\frac{1}{fT_{2p}} = \frac{C^6}{r^6}(f(\tau_c)) \quad (1)$$

where f = [doxyl-DHT]/[isomerase], C is a known constant, and $f(\tau_c)$ is the correlation function. Substituting and taking reciprocals, we may write

$$\frac{[\text{doxyl-DHT}]_{50}^{corr}}{[\text{isomerase}]}(T_{2p}) = \left(\frac{r^6}{C^6}\right)\left(\frac{1}{f(\tau_c)}\right) \quad (2)$$

Since the concentration of isomerase and the correlation function are constant in these titrations and T_{2p} is equalized for all affected NH signals at a spin-label concentration equal to [doxyl-DHT]$_{50}^{corr}$, they may be incorporated into a new constant

$$k = \frac{[\text{isomerase}]}{C^6 T_{2p} f(\tau_c)} \quad (3)$$

such that

$$[\text{doxyl-DHT}]_{50}^{corr} = kr^6 \quad (4)$$

Because this analysis neglects paramagnetic effects of the spin-label on T_1 of the NH signals, which are much smaller but which would also attenuate the NH cross peaks due to decoupling (Villafranca & Mildvan, 1972), only qualitative structural conclusions are drawn.

Table 3 summarizes the values of [doxyl-DHT]$_{50}^{corr}$, and Figure 12 shows 1/[doxyl-DHT]$_{50}^{corr}$ as a function of residue number. The values of [doxyl-DHT]$_{50}^{corr}$ indicate that while many residues are affected by the spin-label, they may be grouped according to the magnitude of the effects. Very strong paramagnetic effects ([doxyl-DHT]$_{50}^{corr}$ < 50 μM) occur on residues 58−61 at the end of helix 3 and on residues 84, 85, and 95 which are adjacent on β-strands 5 and 6 of the β-sheet (Figure 8D). Strong effects (100 μM $\geq$ [doxyl-DHT]$_{50}^{corr}$ $\geq$ 51 μM) are also found on the side chain NH_2 of Asn-57 in helix-3 and on residues of β-strand 3, as well as on residues of β-strands 5 and 6, of the β sheet (Figure 8D). Medium effects (250 μM $\geq$ [doxyl-DHT]$_{50}^{corr}$ $\geq$ 101 μM) are found on helix 3 and β-strands 3, 5, 6, and 7, and weak effects ([doxyl-DHT]$_{50}^{corr}$ > 250 μM) are also found on β-strands 3 and 7 (Table 3, Figure 12). Figure 11B summarizes the residues, and Figure 8D shows backbone ^{15}N and NH regions of the secondary structure which show very strong and strong paramagnetic effects of doxyl-DHT.

From these studies, a self-consistent location of the D ring of the bound steroid is found, near the carboxyl half of helix

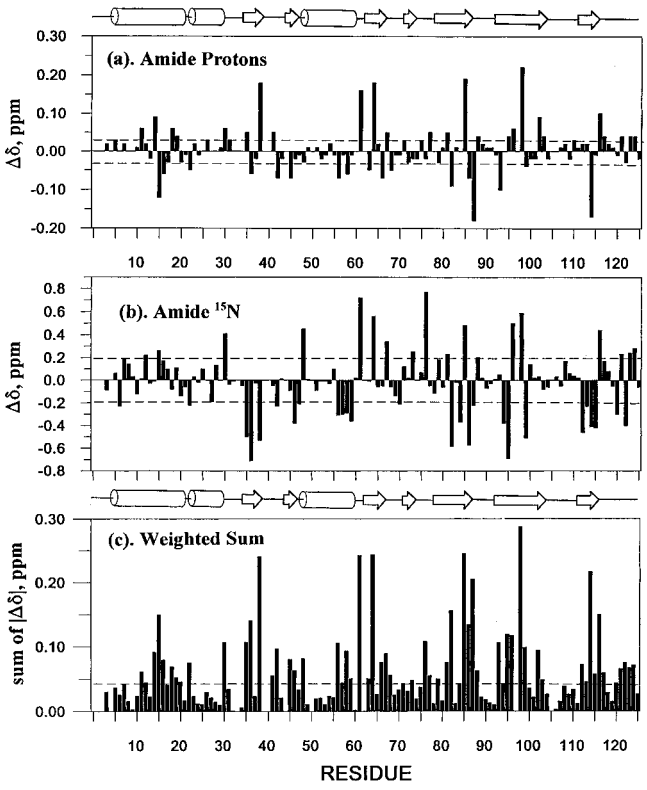

FIGURE 9: Chemical shift changes of the backbone amides of isomerase induced by binding of a product analog, 19-nortestosterone hemisuccinate. The changes ($\Delta\delta = \delta$[adduct] $- \delta$[free]) for amide protons (a) and amide ^{15}N nuclei (b) are shown versus the residue number. The weighted sum (c) of the total chemical changes for both nuclei are calculated by normalizing the $\Delta\delta(^{15}N)$ to the $\Delta\delta(^{1}H)$ with a factor of 8.78, which is the ratio of the backbone amide chemical shift dispersion in the nitrogen and proton dimensions (27.3 and 3.11 ppm). This factor approximates the ratio of gyromagnetic ratios for proton and for nitrogen (9.87).

3 and near one end of the β-sheet. These results with doxyl-DHT (Figure 8D) are consistent with the intermolecular NOE's between 19-NTHS and isomerase (Figure 8C) which place the D ring of the steroid near β-strands 5, 6, and 7 and the C ring near helix 3 and β-strands 3, 5, and 6 of the β-sheet. Like the NOE studies, the paramagnetic effects of doxyl-DHT on isomerase (Table 3, Figure 8D) require the enzyme to be folded in a manner which places helix 3 near the four-stranded β-sheet to satisfy the observed proximities simultaneously. It is of interest that doxyl-DHT affects the same regions of the enzyme that showed changes in ^{15}N and NH chemical shifts on steroid binding except for helix 1 (residues 5−21) and the β-hairpin (residues 34−47) (Table 3, Figure 8). These regions show only chemical shift changes but no paramagnetic effects because of their greater distance from the D ring of the bound steroid. Because it contains Tyr-14, the general acid, helix 1 is near the A ring of the bound steroid substrate. Similarly, because it contains Asp-38, the general base, the β-hairpin is close to both the A and B rings of the enzyme-bound steroid substrate.

DISCUSSION

The overall solution structure of steroid-bound isomerase is very compact, consisting of 30% helices, 38% β-strands, and 16% β-turns. The remaining 16% are assumed to be coils. The high content of periodic secondary structure of this enzyme is consistent with its resistance to digestion by proteolytic enzymes in the absence of denaturants (Benson et al., 1971) and with the unusually slow exchange rate of some of its NH protons (Benisek & Ogez, 1982; Kuliopulos et al., 1987). The high helical content found by NMR differs by 22% from the value of 8% helix estimated from the partially refined crystal structure (Westbrook et al., 1984; Kuliopulos et al., 1987) which was interpreted to show only one 10-residue α-helix from residues 8 to 17. This α-helix overlaps with helix 1 from residues 5 to 21 found by NMR. This difference may explain why further refinement of the X-ray structure was unsuccessful. The overall secondary structure of isomerase is similar to that of a mechanistically related enzyme, β-hydroxydecanoyl thiol ester dehydrase−isomerase (Leesong et al., 1996).

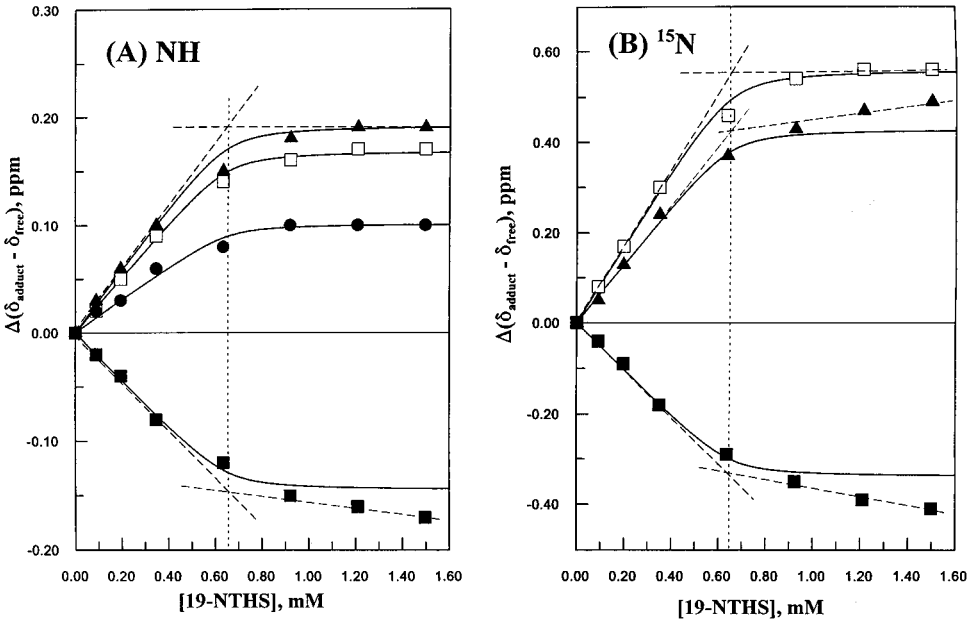

FIGURE 10: Chemical shift titrations of backbone amide protons and nitrogens of some typical residues, Tyr-14 (●) in helix 1, Ala-64 (□) in β-strand 3, Ser-85 (▲) in β-strand 5, and Ala-114 (■) in β-strand 7, as a function of the concentration of 19-NTHS. Panels: (A) chemical shift changes in the proton dimension; (B) chemical shift changes in the nitrogen dimension. All titration curves show 1:1 stoichiometry between the enzyme (0.65 mM in subunit) and ligand, as indicated by the vertical dashed lines. While it is not possible to derive an accurate dissociation constant in this concentration range, the curves generated with a K_D value of 10 μM obtained by kinetic analysis (Zhao et al., 1996a) agree with the titration data.

Table 2: Intermolecular NOE's from Δ^5-3-Ketosteroid Isomerase to 19-NTHS[a]

steroid protons			
location	chemical shift (ppm)	enzyme resonances (δ ^{1}H/δ ^{13}C, ppm) and assignments[b]	secondary structural location[c]
ring A			
1β, 10β	2.22	0.95/22.78, Val-84 γMe$_2$; 1.04/23.25, Val-84 γMe$_1$; 0.71/23.89, *Leu-18* δMe$_1$; 0.93/22.45, Val-95 γMe$_1$; 0.27/21.43, Val-95 γMe$_2$; 0.73/25.65, Leu-59 δMe$_2$; 0.92/23.87, Leu-59 δMe$_1$	H3, β5, β6
2α, 2β	2.35	6.74 Tyr-14 H$_\epsilon$[d]	H1
ring B			
7α	1.03	0.93/22.45, Val-95 γMe$_1$; 0.27/21.43, Val-95 γMe$_2$; 0.95/22.78, Val-84 γMe$_2$; 1.04/23.25, Val-84γMe$_1$	β5, β6
9α	0.87	1.04/23.25, Val-84 γMe$_1$; 0.95/22.78, Val-84 γMe$_2$; 0.27/21.43, Val-95 γMe$_2$; 0.93/22.45, Val-95 γMe$_1$; 0.58/23.34, Leu-63 δMe$_2$; 0.71/26.02, Leu-63 δMe$_1$	β3, β5, β6
ring C			
8β	1.44	1.04/23.25, Val-84 γMe$_1$; 0.95/22.78, Val-84 γMe$_2$; 0.27/21.43, Val-95 γMe$_2$; 0.93/22.45, Val-95 γMe$_1$	β5, β6
12β	1.71	0.93/22.45, Val-95 γMe$_1$; 0.27/21.43, Val-95 γMe$_2$; 0.95/22.78, Val-84 γMe$_2$; 1.04/23.25, Val-84 γMe$_1$; 0.58/23.34, Leu-63 δMe$_2$; 0.71/26.02, Leu-63 δMe$_1$; 0.63/25.97, Leu-*61* δMe$_2$; 0.81/23.97, Leu-*61* δMe$_1$	L(H3$-\beta$3), β3, β5, β6
ring D			
14α	1.09	0.93/22.45, Val-95 γMe$_1$; 0.27/21.43, Val-95 γMe$_2$; 0.95/22.78, Val-84 γMe$_2$; 1.04/23.25, Val-84 γMe$_1$; 0.58/23.34, Leu-63 δMe$_2$; 0.71/26.02, Leu-63 δMe$_1$	β5, β6
16α	2.06	0.93/22.45, Val-95 γMe$_1$; 0.27/21.43, Val-95 γMe$_2$; 0.95/22.78, Val-84 γMe$_2$; 1.04/23.25, Val-84 γMe$_1$; 0.98/14.16, Ile-121 γMe; 0.79/17.52, Ile-121 δMe	β5, β6
18-CH$_3$	0.83	1.04/23.25, Val-84 γMe$_1$; 0.95/22.78, Val-84 γMe$_2$; 0.27/21.43, Val-95 γMe$_2$; 0.93/22.45, Val-95 γMe$_1$; 0.58/23.34, Leu-63 δMe$_2$; 0.71/26.02, Leu-63 δMe$_1$; 0.87/22.31, Thr-93 γMe; 0.63/25.97, Leu-61 δMe$_2$; 0.81/23.97, Leu-61 δMe$_1$; 0.98/14.16, Ile-121 γMe; 0.79/17.52, Ile-121 δMe; *aromatic* 6.98, Phe-86 H$_\epsilon$; 6.80, Phe-86 H$_\delta$; 7.37, Phe-88 H$_{\epsilon/\zeta}$	L(H3$-\beta$3), β3, β5, β6
succinyl			
21-CH$_2$	2.53	0.64/26.02, Leu-61 δMe$_2$; 0.81/23.94, Leu-61 δMe$_1$; 0.79/17.47, Ile-121 δMe; 0.98/14.16, Ile-121 γMe; 0.87/22.31, Thr-93 γMe; 0.93/22.45, Val-95 δMe$_1$; 0.27/21.35, Val-95 γMe$_2$; 0.95/22.78, Val-84 γMe$_2$; 1.04/23.26, Val-84 γMe$_1$; *aromatic* 6.98, Phe-86 H$_\epsilon$; 7.37, Phe-88 H$_{\epsilon/\zeta}$; 6.80, Phe-86 H$_\delta$	L(H3$-\beta$3), β5, β6
22-CH$_2$	2.41	0.64/26.02, Leu-61 δMe$_2$; 0.81/23.94, Leu-61 δMe$_1$; 0.98/14.16. Ile-121γMe; 0.79/17.47, Ile-121 δMe; 1.52/22.25, Ala-114 βMe; 0.86/22.24, Thr-93, γMe; 0.71/23.89, Leu-18 δMe$_1$; 0.47/26.65, Leu-18 δMe$_2$; 0.92/22.52, Val-95 γMe$_1$; 0.29/21.43, Val-95 γMe$_2$; 2.17/20.26, Met-112 ϵMe; 0.96/22.74, Val-84 γMe$_2$; 1.04/23.29, Val-84, γMe$_1$; *aromatic* 7.37, Phe-88 H$_{\epsilon/\zeta}$; 6.98, Phe-86 H$_\epsilon$; 6.80, Phe-86 H$_\delta$	L(H3$-\beta$3), β5, β6, β7

[a] With large amounts of active enzyme in ^2H_2O, exchange of the 2α, 2β, 4, 6α, and 6β steroid protons occurs. The NOE's from Tyr-14 H$_\epsilon$ to the 2α and 2β protons were previously detected in H_2O (Kuliopulos et al., 1991). [b] Effects are listed in order of decreasing magnitude. [c] H refers to helix, β refers to strand, T refers to turn, and L refers to loop and its location. [d] From Kuliopulos et al. (1991).

The ^{15}N and NH resonances of the six amino terminal residues are absent or very weak, probably because of rapid NH exchange with the solvent, as also found by strong exchange cross peaks to water in the NOESY-HSQC spectra. These findings are consistent with the observation that genetic truncation of the first six residues does not significantly affect the catalytic activity of isomerase, suggesting that this region is not important for catalysis or for structure.[5] Because of its location, Phe-88, the first residue of the type II β-turn which caps the antiparallel β-strands 5 and 6, is expected to be exposed to solvent. Such exposure is suggested by the absence of NOE's to its Hα and by the fluorescence properties of a tyrosine at this position (Wu et al., 1994). The sequence consisting of residues 105−110 begins with an apparent type I β-turn between residues 105 and 108 which is exposed and possibly mobile since the NH cross peak for Gly-105 is not seen in the ^{1}H−^{15}N HSQC spectra, and the signals of the adjacent residues (106−108) are very weak due to exchange as confirmed by solvent exchange cross peaks in ^{1}H−^{15}N NOESY-HSQC spectra (data not shown). The side chain NH$_2$ (δ) resonances of Asn-120 are also very weak, and these two proton resonances are shifted from each other by 2.03 ppm (^{1}H, 9.55 and 7.52 ppm; ^{15}N, 111.81 ppm) while the average difference for the other eight side chain amides is only 0.58 ± 0.20 ppm. The large $\Delta\delta$ may be due to the proximity of aromatic residues from β-strands 5 and 6 as suggested by long-range NOE's (data not shown). Similar effects were found for Asn-119 of the Mut T enzyme, and the solution structure reveals this residue to be surrounded by aromatic side chains (Abeygunawardana et al., 1995).

The substrate binding site of isomerase has been located by three independent NMR methods: (i) diamagnetic effects of 19-NTHS binding on backbone NH and ^{15}N chemical shifts of the enzyme, (ii) intermolecular NOE's between 19-NTHS and assigned resonances of the enzyme, and (iii) paramagnetic effects of doxyl-DHT on the intensities of assigned backbone and side chain NH and ^{15}N cross peaks of the enzyme. While the latter two methods are distance dependent, hence more reliable, all three of these methods independently showed the importance of the carboxy-terminal half of helix 3 and β-strands 3, 5, 6, and 7 of the antiparallel β-sheet in steroid binding (Figure 8, Table 3). In addition, the intermolecular NOEs and the chemical shift changes indicated the participation of helix 1 (which contains Tyr-14), and the chemical shift changes indicated the participation of the β-hairpin (which contains Asp-38) in steroid binding. To satisfy the proximities detected by both

[5] Q. Zhao and P. Talalay, unpublished observations, 1994.

Table 3: Concentrations of Doxyl-DHT Required To Decrease HSQC Cross Peak Intensities by 50% ([Doxyl-DHT]$_{50}^{corr}$) for Various Backbone and Side Chain Amide Resonances

residues[a]	chemical shift (ppm) ^{1}H	chemical shift (ppm) ^{15}N	[doxyl-DHT]$_{50}$ (μM)	initial relative intensity	[doxyl-DHT]$_{50}^{corr}$ (μM)	category[b]	secondary structure location[c]
Ser-58	7.65	118.77	9.4	1.58	14.9 ± 1.6	very strong	H3
Leu-59	7.38	119.58	15.5	1.51	23.4 ± 1.8	very strong	H3
Lys-60	7.10	120.53	11.4	1.62	18.5 ± 1.6	very strong	H3
Leu-61	7.44	120.27	8.2	1.78	14.6 ± 0.6	very strong	L(H3−β3)
Val-84	9.07	122.87	19.3	1.27	24.5 ± 6.1	very strong	β5
Ser-85	9.20	123.18	28.0	1.24	34.7 ± 5.0	very strong	β5
Val-95	9.38	130.01	20.2	1.80	36.4 ± 6.3	very strong	β6
Asn-57							
NHδ1	7.58	115.71	38.0	1.87	71 ± 16	strong	H3
NHδ2	6.98	115.71	42.0	2.04	86 ± 9	strong	H3
Leu-63	8.32	125.05	57.0	1.31	75 ± 14	strong	β3
Phe-86	8.43	121.35	48.0	1.53	74 ± 12	strong	β5
Thr-93	8.76	126.29	68.0	1.31	89 ± 12	strong	β6
Ala-96	8.35	132.17	94.0	1.07	100 ± 23	strong	β6
Phe-55	8.57	121.12	95.0	1.21	115 ± 27	medium	H3
Ala-56	8.99	125.52	98.0	1.57	154 ± 29	medium	H3
Ala-64	8.47	124.51	80.0	1.31	105 ± 48	medium	β3
Val-94	8.53	127.34	81.0	1.47	119 ± 31	medium	β6
Asp-99	8.29	126.14	119.0	1.05	125 ± 24	medium	β6
Ala-114	8.34	128.89	91.0	1.15	105 ± 31	medium	β7
Phe-116	6.80	118.87	142.0	1.29	183 ± 55	medium	β7
Gly-21	7.83	111.38	345.0	1.00	345 ± 53	weak	H1
Val-65	10.02	130.34	255.0	1.21	310 ± 64	weak	β3
Glu-66	8.60	127.76	257.0	1.41	364 ± 75	weak	β3
Gln-89							
NHϵ1	7.01	112.98	106.0	2.66	282 ± 57	weak	T5
NHϵ2	6.69	112.98	150.0	2.26	339 ± 48	weak	T5
Gly-117	9.16	111.61	250.0	1.25	313 ± 131	weak	L(β7−T5)
					very weak, [doxyl-DHT]$_{50}^{corr}$ ≥ 401 μM		
Gln-12, Tyr-14, Ala-16, Leu-18, Ser-42, Arg-72, Ala-78, Ala-79, Arg-91, Phe-103, Ile-121, His-122							

[a] Asp-38 is also very weakly affected but the [doxyl-DHT]$_{50}^{corr}$ could not be quantitated because of spectral overlap with the NH resonance of Ala-73. [b] Categories of paramagnetic effects are defined as follows: very strong, [doxyl-DHT]$_{50}^{corr}$ < 50 μM; strong, 51 μM ≤ [doxyl-DHT]$_{50}^{corr}$ ≤ 100 μM; medium, 101 μM ≤ [doxyl-DHT]$_{50}^{corr}$ ≤ 250 μM; weak, 251 μM ≤ [doxyl-DHT]$_{50}^{corr}$ ≤ 400 μM; very weak, [doxyl-DHT]$_{50}^{corr}$ ≥ 401 μM. [c] H refers to helix, β refers to strand, T refers to turn, and L refers to loop and its location.

the NOE's and the paramagnetic effects, helices 1 and 3 must be near the hydrophobic face of the β-sheet in the tertiary structure of isomerase.

Ring A of the steroid approaches Tyr-14 as previously found by NOE's between Hϵ of Tyr-14 and the 2α- and 2β-protons of 19-NTHS (Kuliopulos et al., 1991). The junction between the A and B rings is positioned near Asp-38, the catalytic base, as inferred from site-directed mutagenesis (Kuliopulos et al., 1989), affinity labeling (Kayser et al., 1983), and chemical modification studies (Benisek et al., 1980), and near Asn-57, as found by affinity labeling (Penning & Talalay, 1981). Efficient relaxation of the side chain NH_2 of Asn-57 by doxyl-DHT provides independent evidence for the proximity of this side chain to the bound steroid. The presence of the catalytic residue Asp-38 in a structured β-hairpin and Tyr-14 in a structured α-helix rather than in more flexible loops or turns is unusual and is consistent with the 340-fold decrease in activity resulting from the conservative D38E mutation (Zawrotney & Pollack, 1994). Moreover, this mutation has also been found to increase solvent proton exchange into the reaction product, indicating that this small structural modification loosens the structure near the active site.

The extensive four-stranded antiparallel β-sheet structure, a portion of which forms one surface of the active site, contains many hydrophobic residues including seven phenylalanine, four valine, two leucine, and three alanine residues on the *same face*, presumably to exclude water. The other surface of the active site is formed by helix 1, which contains Tyr-14, the β-hairpin which contains Asp-38, and

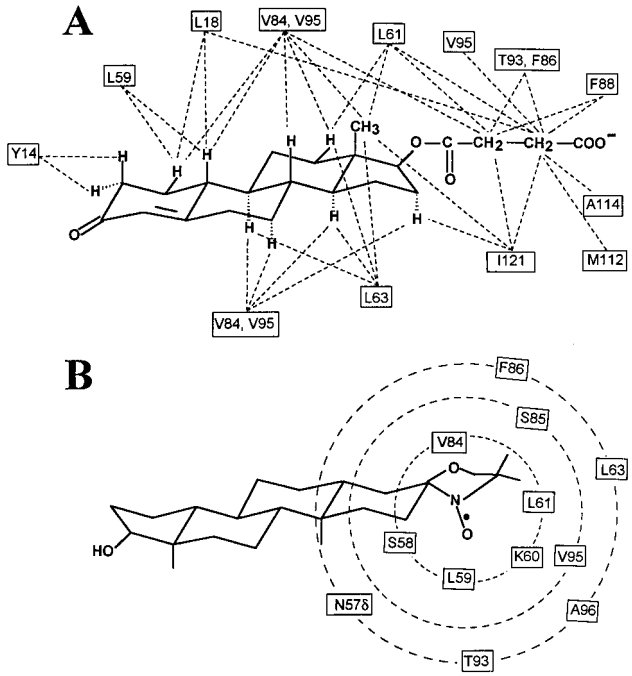

FIGURE 11: Active site residues of isomerase in close proximity to bound steroids. (A) Residues showing intermolecular NOE's from isomerase protons to protons of 19-NTHS. The NOE's from Tyr-14 to 19-NTHS were previously reported (Kuliopulos et al., 1991). (B) Residues of isomerase showing *very strong* and *strong* paramagnetic effects of doxyl-DHT on backbone ^{15}N and NH cross peaks in ^{1}H−^{15}N HSQC spectra. The inner shell shows residues which have [doxyl-DHT]$_{50}^{corr}$ < 25 μM. The second shell shows residues with 25 μM ≤ [doxyl-DHT]$_{50}^{corr}$ ≤ 50 μM. The third shell shows residues with 51 μM ≤ [doxyl-DHT]$_{50}^{corr}$ ≤ 100 μM.

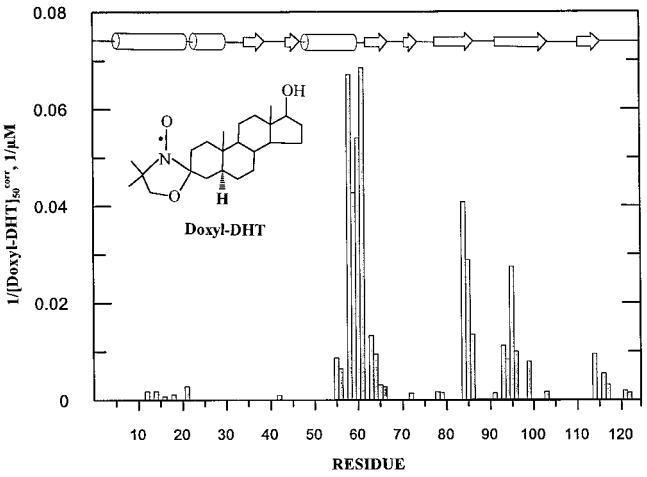

FIGURE 12: Histogram showing paramagnetic effects of doxyl-DHT on ^{15}N and NH resonances of isomerase. The reciprocal of [doxyl-DHT]$_{50}^{corr}$ is plotted against residue number. Also shown are the regions of secondary structure of isomerase.

helix 3 which contains Asn-57 and is strongly relaxed by doxyl-DHT. Such a hydrophobic structure is consistent with the low dielectric constant of ~18 at the active site (Li et al., 1993), with the ~95% conservation of the proton transferred by Asp-38 from the 4β- to the 6β-position of the steroid during catalysis (Wang et al., 1963; Hawkinson et al., 1991), and with the slow exchange and inaccessibility to H_3O^+ or OH^- of the strongly hydrogen bonded Tyr-14 OH proton in the reaction intermediate (Zhao et al., 1996b).

With the NMR-corrected secondary structure of Δ^5-3-ketosteroid isomerase in hand, the tertiary structure of this homodimeric enzyme can, in principle, be solved by X-ray, by refitting the electron density map, and by NMR, provided that the interface between the subunits can be unequivocally established. Such structural information, together with the more precise location of the steroid binding site, will give greater insight into the catalytic mechanism of this efficient isomerase—a prototype enzyme for the catalysis of enolizations and allylic rearrangements.

ACKNOWLEDGMENT

We thank Dr. Paul Talalay for advice and encouragement throughout the course of this work, Dr. David Gorenstein of the University of Texas, Galveston, for providing us time on the Varian Unityplus 750 spectrometer, Dr. Jian Lin for useful discussions and for providing a computer program for analyzing the HSQC titration data, and Gale Doremus for help in preparing the manuscript.

SUPPORTING INFORMATION AVAILABLE

Two tables giving resonance assignments in the Δ^5-3-ketosteroid isomerase−19-NTHS complex (Table S1) and changes in ^{15}N and NH chemical shifts of isomerase on binding of 19-NTHS (Table S2) and one figure showing chemical shift indices of backbone Hα, Cα, Cβ, and C=O resonances (Figure S1) (13 pages). Ordering information is given on any current masthead page.

REFERENCES

Abeygunawardana, C., Weber, D. J. Frick, D. N., Bessman, M. J., & Mildvan, A. S. (1993) *Biochemistry 32*, 13071−13080.

Abeygunawardana, C., Weber, D. J., Gittis, A. G., Frick, D. N., Lin, J., Miller, A.-F., Bessman, M. J., & Mildvan, A. S. (1995) *Biochemistry 34*, 14997−15005.

Abeygunawardana, C., Mori, S., Van Zihl, P. C. M., & Mildvan, A. S. (1996) *34th Experimental NMR Conference*, Pacific Grove, CA, Abstract WP4, p 224.

Austin, J. C., Zhao, Q., Jordan, T., Talalay, P., Mildvan, A. S., & Spiro, T. G. (1995) *Biochemistry 34*, 4441−4447.

Bax, A., Clore, G. M., & Gronenborn, A. M. (1990) *J. Magn. Reson. 88*, 425−431.

Benisek, W. F., & Ogez, J. R. (1982) *Biochemistry 21*, 5816−5825.

Benisek, W. F., Ogez, J. R., & Smith, S. B. (1980) *Ann. N.Y. Acad. Sci. 346*, 115−130.

Benson, A. M., Jaraback, R., & Talalay, P. (1971) *J. Biol. Chem. 246*, 7514−7525.

Benson, A. M., Suruda, A. J., & Talalay, P. (1975) *J. Biol. Chem. 250*, 276−280.

Bodenhausen, G., & Ruben, D. J. (1980) *Chem. Phys. Lett. 69*, 185−188.

Eames, T. C., Hawkinson, D. C., & Pollack, R. M. (1990) *J. Am. Chem. Soc. 112*, 1996−1998.

Ebrahimian, S., Starich, M. R., Perez-Alvarado, G. C., Summers, M. F., & Pollack, R. M. (1995) *FASEB J. 9*, A1341.

Goodwin, T. W., & Morton, R. A. (1946) *Biochem. J. 40*, 628−632.

Grzesiek, S., & Bax, A. (1993) *J. Biomol. NMR 3*, 185−204.

Hawkinson, D. C., Eames, T. C. M., & Pollack, R. M. (1991) *Biochemistry 30*, 6956−6964.

Holman, C. M., & Benisek, W. F. (1994) *Biochemistry 33*, 2672−2681.

Ikura, M., Bax, A., Clore, G. M., & Gronenborn, A. M. (1990) *J. Am. Chem. Soc. 112*, 9020−9022.

Kawahara, F. S., & Talalay, P. (1960) *J. Biol. Chem. 235*, PC1-2.

Kay, L. E., Clore, G. M., Bax, A., & Gronenborn, A. M. (1990a) *Science 249*, 411−414.

Kay, L. E., Ikura, M., Tschudin, R., & Bax, A. (1990b) *J. Magn. Reson. 89*, 496−514.

Kay, L. E., Xu, G.-Y., Singer, A. U., Muhandiram, D. R., & Forman-Kay, J. D. (1993) *J. Magn. Reson. 101B*, 333−337.

Kay, L. E., Xu, G.-Y., & Yamazaki, T. (1994) *J. Magn. Reson. 109A*, 129−133.

Kayser, R. H., Bounds, P. L., Bevins, C. L., & Pollack, R. M. (1983) *J. Biol. Chem. 258*, 909−915.

Kuliopulos, A., Shortle, D., & Talalay, P. (1987a) *Proc. Natl. Acad. Sci. U.S.A. 84*, 8893−8897.

Kuliopulos, A., Westbrook, E. M., Talalay, P., & Mildvan, A. S. (1987b) *Biochemistry 26*, 3927−3937.

Kuliopulos, A., Mildvan, A. S., Shortle, D., & Talalay, P. (1989) *Biochemistry 28*, 149−159.

Kuliopulos, A., Talalay, P., & Mildvan, A. S. (1990) *Biochemistry 29*, 10271−10280.

Kuliopulos, A., Mullen, G. P., Xue, L., & Mildvan, A. S. (1991) *Biochemistry 30*, 3169−3178.

Lee, W., Revington, M. J., Arrowsmith, C., & Kay, L. E. (1994) *FEBS Lett. 350*, 87−90.

Lee, W., Revington, M. J., Farrow, N. A., Nakamura, A., Utsunomiya-Tate, N., Miyake, Y., Kainosho, M., & Arrowsmith, C. H. (1995) *J. Biomol. NMR 5*, 367−375.

Leesong, M., Henderson, B. S., Gillig, J. R., Schwab, J. M., & Smith, J. L. (1996) *Structure 4*, 253−264.

Levy, G. C., & Lichter, R. L. (1979) *Nitrogen-15 Nuclear Magnetic Resonance Spectroscopy*, John Wiley & Sons, New York.

Li, Y.-K., Kuliopulos, A., Mildvan, A. S., & Talalay, P. (1993) *Biochemistry 32*, 1816−1824.

Marion, D., & Wüthrich, K. (1983) *Biochem. Biophys. Res. Commun. 113*, 967−974.

Marion, D., Driscoll, P. C., Kay, L. E., Wingfield, P. T., Bax. A., Gronenborn, A. M., & Clore, C. M. (1989) *Biochemistry 28*, 6150−6156.

Mildvan, A. S., & Engle, J. L. (1972) *Methods Enzymol. 26*, 654−682.

Mildvan, A. S., & Gupta, R. K. (1978) *Methods Enzymol 49*, 322−359.

Mori, S., Abeygunawardana, C., Johnson, M. O., & van Zijl, P. C. M. (1995) *J. Magn. Reson. B108*, 94−98.

Muhandiram, D. R., & Kay, L. E. (1994) *J. Magn. Reson. B103*, 203−216.

Muhandiram, D. R., Farrow, N. A., Xu, G.-Y., Smallcombe, S. H., & Kay, L. E. (1993) *J. Magn. Reson. 102B*, 317−321.

Neidhardt, F. C., Bloch, P. L., & Smith, D. F. (1974) *J. Bacteriol. 119*, 736−747.
Pascal, S. M., Muhandiram, D. R., Yamazaki, T., Forman-Kay, J. D., & Kay, L. E. (1994) *J. Magn. Reson. 103B*, 197−201.
Penning, T. M., & Talalay, P. (1981) *J. Biol. Chem. 265*, 6851−6858.
Schwab, J. M., & Henderson, B. S. (1990) *Chem. Rev. 90*, 1203−1245.
Spera, S., & Bax, A. (1991) *J. Am. Chem. Soc. 113*, 5490−5492.
Viger, A., Coustal, S., & Marquet, A. (1981) *J. Am. Chem. Soc 103*, 451−458.
Villafranca, J. J., & Mildvan, A. S. (1972) *J. Biol. Chem. 247*, 3454−3463.
Vuister, G. W., & Bax, A. (1992) *J. Magn. Reson. 98*, 428−435.
Wang, S.-F., Kawahara, F. S., & Talalay, P. (1963) *J. Biol. Chem. 258*, 576−585.
Westbrook, E. M., Piro, O. E., & Sigler, P. B. (1984) *J. Biol. Chem. 259*, 9096−9103.
Wishart, D. S., & Sykes, B. D. (1994) *J. Biomol. NMR 4*, 171−180.
Wishart, D. S., Sykes, B. D., & Richards, F. M. (1991) *J. Mol. Biol. 222*, 311−333.
Wishart, D. S., Sykes, B. D., & Richards, F. M. (1992) *Biochemistry 31*, 1647−1651.
Wittekind, M., & Mueller, L. (1993) *J. Magn. Reson. B101*, 201−205.
Wu, P., Li, Y.-K., Talalay, P., & Brand, L. (1994) *Biochemistry 33*, 7415−7422.
Wüthrich, K. (1986) *NMR of Proteins and Nucleic Acids*, pp 162−175, John Wiley & Sons, Inc., New York.
Xue, L., Talalay, P., & Mildvan, A. S. (1990) *Biochemistry 29*, 7491−7500.
Xue, L., Kuliopulos, A., Mildvan, A. S., & Talalay, P. (1991) *Biochemistry 30*, 4991−4997.
Zawrotney, M. E., & Pollack, R. M. (1994) *Biochemistry 33*, 13896−13902.
Zhang, O., Kay, L. E., Olivier, P. J., & Forman-Kay, J. D. (1994) *J. Biomol. NMR 4*, 845−858.
Zhao, Q., Mildvan, A. S., & Talalay, P. (1995a) *Biochemistry 34*, 426−434.
Zhao, Q., Li, Y.-K., Mildvan, A. S., & Talalay, P. (1995b) *Biochemistry 34*, 6562−6572.
Zhao, Q., Abeygunawardana, C., & Mildvan, A. S. (1996a) *Biochemistry 35*, 1525−1532.
Zhao, Q., Abeygunawardana, C., Talalay, P., & Mildvan, A. S. (1996b) *Proc. Natl. Acad. Sci. U.S.A. 93*, 8220−8224.

BI962844U